Automatica 111 (2020) 108640

Contents lists available at ScienceDirect

Automatica

journal homepage: www.elsevier.com/locate/automatica

Adaptive output-feedback control of torsional vibration in off-shore rotary oil drilling systems☆

Ji Wang [a], Shu-Xia Tang [b,*], Miroslav Krstic [a]

[a] Department of Mechanical and Aerospace Engineering, University of California, San Diego, La Jolla, CA 92093-0411, USA
[b] Department of Mechanical Engineering, Texas Tech University, Lubbock, TX 79409, USA

ARTICLE INFO

Article history:
Received 31 July 2018
Received in revised form 20 March 2019
Accepted 13 September 2019
Available online 8 November 2019

Keywords:
Wave PDE
Adaptive output-feedback control
Backstepping
Anti-collocated disturbance
Oil drilling

ABSTRACT

Motivated by an engineering application of torsional vibration suppression of off-shore oil drilling, we design an adaptive output-feedback controller for a one-dimensional wave partial differential equation (PDE) system, where an anti-damping term with an unknown coefficient and a general harmonic disturbance with unknown amplitudes exist in the bit, which is modeled as a second-order-in-time boundary. The control input anti-collocated with this boundary subject to uncertainty, is designed by using the adaptive control method and infinite-dimensional backstepping technique. The asymptotic convergence to zero of the uncontrolled boundary states, i.e., the oscillations of the angular displacement and velocity at the bit, and the boundedness of all states in the closed-loop system, are proved via Lyapunov analysis. The effectiveness of the proposed adaptive controller is verified via numerical simulation. The results also can be applied to other applications, such as vibration control of cable elevators with uncertain cage-guide friction and cage disturbances.

1. Introduction

1.1. Vibrations in oil drilling system

Oil drilling systems used to drill deep boreholes for hydrocarbon exploration and production often suffer severe vibrations, which would cause premature failure of drilling string components, damage to the borehole wall, and problems to precise control (Jansen, 1993). Besides, the vibrations also cause significant wastage of drilling energy (Dunayevsky, Abbassian, & Judzis, 1993). Suppression of vibrations in the oil drilling system is thus required considering the economic interest and improvement of drilling performance (Saldivar, Mondiš, Niculescu, Mounier, & Boussaada, 2016).

There are three main types of vibrations in oil drilling systems (Saldivar, Boussaada, Mounier, & Mondie, 2014): vertical vibration, also called the bit-bouncing phenomenon, lateral vibration due to the out-of-balance of the drill string, which is called whirl motion, and torsional vibration which appears due to the friction between the bit and the rock. This nonlinear torsional interaction between the drill bit and the rock would cause the bit to slow down and even stall while the rotary table is still in motion. Once enough energy has been accumulated, the bit would be suddenly released and starts rotating at very high speed before slowing down again (Bresch-Pietri & Krstic, 2014a), settling into a limit cycling motion. This is called the stick–slip phenomenon. The stick–slip oscillations would lead to the instability from the lower end traveling up to the drill string and the rotatory table, which results in distributed instabilities and primarily provokes fatigue to drill collar connections and damages the drill bit (Saldivar et al., 2014). Therefore, suppressing torsional vibrations (stick–slip oscillations) in the oil drilling system is important and is the focus of this article. In addition to the stick–slip instability, wave at the sea surface, causing heaving motion of the drilling rig (Aamo, 2013) in an off-shore rotary oil drilling system would introduce an external disturbance at the bit. The control task in this article is to deal with the stick–slip instability and external disturbances at the same time to asymptotically stabilize the oscillations of the vibrational angular displacement and velocity at the drill bit.

1.2. Oil drilling vibration models

One category of existing drilling models used for the control design is a lumped parameter model, where the drill string is approximated as a mass–spring–damper system described by an ordinary differential equation (ODE). Based on this model, the traditional ODE control strategies are used to suppress vibrations

☆ The material in this paper was not presented at any conference. This paper was recommended for publication in revised form by Associate Editor Peng Shi under the direction of Editor Thomas Parisini.

* Corresponding author.
E-mail addresses: jiw248@eng.ucsd.edu (J. Wang), shuxia.tang@ttu.edu (S.-X. Tang), krstic@ucsd.edu (M. Krstic).

https://doi.org/10.1016/j.automatica.2019.108640
0005-1098/

in Germay, Van De Wouw, Nijmeijer, and Sepulchre (2005) and Richarda, Germayb, and Detournay (2007). Another category is a neutral-type time-delay model (Abolinia & Myshkis, 1960), where a pair of delay differential equations is derived to describe an equivalent input–output model, and then several stabilizing control laws are designed based on the attractive ellipsoid method (Saldivar & Mondiš, 2013) and Lyapunov theory (Saldivar, Mondiš, Loiseau, & Rasvan, 2013). Even though the use of the lumped parameter model and the neutral-type time-delay model simplifies the control system design, they neglected the distributed nature of the system (Saldivar et al., 2016), which may cause the spillover instability (Zhang, He, & Ge, 2012).

An infinite dimensional model describing the torsional vibrations in the drilling string is a wave PDE model (Bresch-Pietri & Krstic, 2014a, 2014b; Sagert, Di Meglio, Krstic, & Rouchon, 2013), where the model spillover phenomenon is avoided (Zhang et al., 2012). In this article, we use the one-dimensional wave PDE to describe the torsional vibration dynamics of the drilling string.

1.3. Models for stick–slip phenomenon and external disturbances

Several physical laws of bit-rock friction (Saldivar et al., 2016) are used to roughly describe the stick–slip behavior in the reduced finite dimensional model of the oil drilling system, such as the velocity weakening law (Challamel, 2000), stiction plus Coulomb friction model (Serrarens, van de Molengraft, Kok, & van den Steeen, 1998), a class of Karnopp model (Detournay & Defourny, 1992; Karnopp, 1985; Navarro-López & Cortés, 2007). In the infinite dimensional model of the oil drilling system, the stick–slip behavior between the bit and rock is usually simplified as a linear anti-damped term, such as Bresch-Pietri and Krstic (2014a, 2014b, 2014c) and Sagert et al. (2013). The coefficient of the anti-damped term depends on some other factors about the nature of the rock and is difficult to be known in advance. In this paper, the stick–slip instability in the wave PDE modeling the drilling string dynamics is described as an anti-damped term with a coefficient being unknown in the second-order-in-time boundary describing the bit dynamics.

The external disturbance at the bit resulted from wave-induced heaving motion of the drilling rig (Aamo, 2013) is usually described by a harmonic form with known frequencies and unknown amplitudes (Landet, Pavlov, & Aamo, 2013), because the amplitudes of the disturbance caused by heave motion may be affected by winds or ocean currents, and are difficult to be defined in advance, while the dominating frequency components of the heave motion of a specific sea area are usually accessible. In this paper, the disturbance at the bit is modeled as the harmonic function with known frequencies and unknown amplitudes.

1.4. Control of wave PDE with anti-collocated instability or disturbances

In the off-shore rotary oil drilling system, a one-dimensional wave PDE describes the torsional vibrations of the drilling string and a second-order-in-time boundary opposite to the control input represents the bit torsional vibration dynamics, including an anti-damping term with an unknown coefficient and a general harmonic function with unknown amplitudes denoting the stick–slip instability and the disturbance at the bit respectively. The control task is thus boundary stabilization of a wave PDE with both high uncertainty and instability at the anti-collocated boundary.

In Krstic, Guo, Balogh, and Smyshlyaev (2008), the boundary stabilization problem of a one-dimensional wave PDE which contains the instability at its free end and the control input on the opposite end was dealt with by using the backstepping method (Krstic & Smyshlyaev, 2008a). In Bekiaris-Liberis and Krstic (2014), the first global stabilization result was achieved for a wave PDE-nonlinear ODE system where the actuator is anti-collocated with the source of the instability. Moreover, for the uncertain anti-collocated instability, adaptive control laws (Krstic, 2009b; Krstic & Smyshlyaev, 2008b) were developed for a one-dimensional wave PDE which had an actuator on one boundary and an anti-damping instability with an unknown coefficient on the other boundary in Bresch-Pietri and Krstic (2014a, 2014b, 2014c). For the anti-collocated disturbance attenuation problem in wave PDEs, output reference tracking of a wave equation with an anti-collocated harmonic disturbance at a stable damping boundary was presented in Guo and Guo (2016). The output regulation problem for a wave equation with a harmonic anti-collocated disturbance at a free boundary was dealt with in Guo, Shao, and Krstic (2017). In Wang, Tang, Pi and Krstic (2018), an output-feedback controller was designed to attenuate an anti-collocated disturbance and exponentially regulate the uncontrolled boundary state of a wave PDE on a time-varying domain based on the backstepping and the active disturbance rejection control (ADRC) approach. However, the boundary control problem of a wave PDE with both instability and disturbance which include unknown coefficients in the boundary anti-collocated with the control, motivated by the application in the oil drilling, is more challenging. Because high uncertainty and instability simultaneously exist in the boundary anti-collocated with the control input, traditional ADRC (Tang, Guo, & Krstic, 2014) cannot be used directly.

1.5. Contributions of the paper

- To the author's best knowledge, it is the first control result of a PDE-modeled oil drilling system considering both the uncertain stick–slip instability and an uncertain harmonic disturbance at the bit.
- Compared with Krstic (2009c) and Sagert et al. (2013) which design boundary control to stabilize a wave PDE coupled with an unstable ODE at the boundary opposite to the control input via backstepping, the main contribution of this paper is in considering the coefficient of the source of instability in the ODE as unknown and in handling an uncertain external disturbance at the ODE, anti-collocated with the control input.
- The novelty of this paper is that an instability term with an unknown coefficient and an uncertain harmonic disturbance at the uncontrolled boundary need to be dealt with simultaneously in a wave PDE, compared with Bresch-Pietri and Krstic (2014a, 2014b) stabilizing a wave PDE including an unknown-coefficient anti-damping term at the boundary anti-collocated with the control input, or Guo et al. (2017) and Wang, Tang et al. (2018) dealing with an anti-collocated uncertain disturbance in a wave PDE.

1.6. Organization

The rest of the paper is organized as follows. We present the torsional vibration dynamics of oil drilling with stick–slip instability and a disturbance at the bit in Section 2. The adaptive update laws for the unknown coefficients are presented in Section 3. The design of the output-feedback controller via the backstepping method is proposed in Section 4. The stability proof of the resulted closed-loop control system is proved in Section 5. Simulation results are provided in Section 6. The conclusion and future work are presented in Section 7.

2. Problem formulation

2.1. A wave PDE model

The off-shore oil drilling system rotates around its vertical axis, penetrating through the rock on the sea floor (see Fig. 1). It consists of the assembly of a drill pipe, a drill collar, and a rock-cutting tool referred to as drill bit. At the top of the drill string, the rotary table provides the necessary torque to push the system into a rotary motion (Sagert et al., 2013). The torsional vibration dynamic model of the rotary off-shore oil drill string system can be written as:

$$u_{tt}(x,t) = qu_{xx}(x,t), \tag{1}$$

$$u_x(L,t) = U(t), \tag{2}$$

$$I_b u_{tt}(0,t) = cu_t(0,t) - ku_x(0,t) - d(t), \tag{3}$$

where the state $u(x,t)$ denotes the distributed elastic angular displacement of the drill pipe; $x \in [0, L]$ with L being the length of the drill pipe; $t \in [0, \infty)$ representing the time. The coefficients $q = GJ/I_d$, $k = GJ$, with G, J, I_d being the shear modulus of the drill pipe, drill pipe second moment of area and drill pipe moment of inertia per unit of length, respectively; I_b is the moment of inertia of the bottom hole assembly (BHA). $U(t)$ is the scalar input and $kU(t)$ represents the control torque in practice. $cu_t(0,t)$ describes the stick–slip instability between the bit and the rock at the bottom. Moreover, $d(t)$ denotes the pressure oscillations on the drill bit caused by wave-induced heaving motion of the drilling rig.

Two assumptions are made for the unknown coefficient c and the uncertain disturbance $d(t)$:

Assumption 1. The anti-damping coefficient c in (3) is unknown but bounded by a known and arbitrary constant $\bar{c}$, i.e., $c \in [0, \bar{c}]$.

Assumption 2. The disturbance $d(t)$ is of the general harmonic form as

$$d(t) = \sum_{j=1}^{N} [a_j \cos(\theta_j t) + b_j \sin(\theta_j t)], \tag{4}$$

where the integer N is an arbitrary integer. The frequencies θ_j are known and arbitrary constants. The amplitudes a_j, b_j are unknown constants bounded by the known and arbitrary constants $\bar{a}_j, \bar{b}_j$, i.e., $a_j \in [0, \bar{a}_j]$, $b_j \in [0, \bar{b}_j]$.

Remark 1. The frequency information requirement is reasonable in the wave-introduced disturbance considered in this paper because the dominant frequency of the ocean waves is usually slowly varying and mostly known for the particular area of the ocean (Fossen, 2011). Actually, even if the frequency information is unavailable in some other application cases, (4) also can model most periodic disturbance signals since N is arbitrary and can be chosen sufficiently large.

The available boundary measurements are:

- The torsional vibration acceleration $u_{tt}(0,t)$ measured by the acceleration sensor placed at the bit
- The torsional vibration velocity $u_t(L,t)$ which can be obtained easily from the feedback signal in the servo actuator.

Note that we obtain the torsional vibration displacement and velocity at the bit $u(0,t), u_t(0,t)$ by twice integrating the measurement $u_{tt}(0,t)$ with known initial conditions $u(0,0), u_t(0,0)$, because the installation of the acceleration sensor is more economic and convenient.

With the coefficient c of the anti-damping term being unknown and the amplitudes a_j, b_j of the harmonic disturbance $d(t)$ being unknown at the uncontrolled boundary $x = 0$, the control objective in this paper is to design a control input $U(t)$ using available boundary measurements to guarantee the asymptotic convergence to the origin of the torsional vibrational angular displacement $u(0,t)$ and velocity $u_t(0,t)$ of the drill bit at the downhole boundary. The uniform boundedness of all states in the closed-loop system should be ensured as well.

2.2. A wave PDE–ODE model

In addition to the challenges from the unknown coefficient in the anti-damping term and the uncertain external disturbance at the uncontrolled boundary, the second order boundary condition (3) which is also anti-collocated with the control input poses difficulties to the control problem as well. To solve this, we define

$$X(t) = [u(0,t), u_t(0,t)]^T, \tag{5}$$

and then the system (1)–(3) can be written as a PDE–ODE coupled (Tang & Xie, 2011; Zhou & Tang, 2012) system:

$$\dot{X}(t) = AX(t) + Bu_x(0,t) + \frac{1}{k}Bd(t), \tag{6}$$

$$u(0,t) = CX(t), \tag{7}$$

$$u_{tt}(x,t) = qu_{xx}(x,t), \tag{8}$$

$$u_x(L,t) = U(t), \tag{9}$$

where

$$A = \begin{bmatrix} 0 & 1 \\ 0 & \frac{c}{I_b} \end{bmatrix}, B = \frac{k}{I_b}\begin{bmatrix} 0 \\ -1 \end{bmatrix}, C = [1, 0]. \tag{10}$$

Note that the second order boundary (3) becomes the first order one now and A is an uncertain matrix including the unknown anti-damping coefficient c. The control objective is thus to ensure the asymptotic convergence of $X(t)$.

2.3. A 2 × 2 transport PDEs–ODE model

In order to reduce the time derivative order of the plant (6)–(9), we use the following Riemann coordinates:

$$z(x,t) = u_t(x,t) - \sqrt{q}u_x(x,t), \tag{11}$$

$$w(x,t) = u_t(x,t) + \sqrt{q}u_x(x,t) \tag{12}$$

to reversibly rewrite the system (6)–(9) as

$$\dot{X}(t) = \left(A - \frac{1}{\sqrt{q}}BC_1\right)X(t) + \frac{1}{\sqrt{q}}Bw(0,t) + \frac{1}{k}Bd(t), \tag{13}$$

$$z(0,t) = 2C_1X(t) - w(0,t), \tag{14}$$

$$z_t(x,t) = -\sqrt{q}z_x(x,t), \tag{15}$$

$$w_t(x,t) = \sqrt{q}w_x(x,t), \tag{16}$$

$$w(L,t) = 2\sqrt{q}U(t) + z(L,t), \tag{17}$$

Note that $q > 0$ according to the definition in Section 2.1, and the state matrix in ODE (13) can be rewritten as

$$A - \frac{1}{\sqrt{q}}BC_1 = A_E + A_c - \frac{1}{\sqrt{q}}BC_1 \tag{18}$$

where

$$C_1 = [0, 1], \tag{19}$$

by defining

$$A_E = \begin{bmatrix} 0 & 1 \\ 0 & 0 \end{bmatrix}, \tag{20}$$

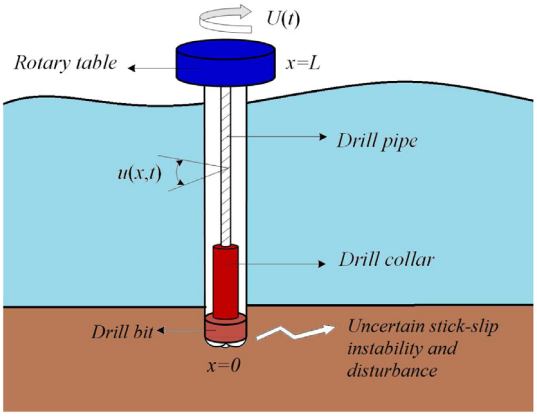

Fig. 1. A drill string used in offshore oil drilling. $u(x,t)$ denotes the distributed elastic angular displacement of the drill string. The drill bit is subjected to the uncertain stick–slip instability and disturbance, which are anti-collocated with the torque $U(t)$ at the rotary table.

$$A_c = A - A_E = \begin{bmatrix} 0 & 0 \\ 0 & \frac{c}{I_b} \end{bmatrix}, \tag{21}$$

which will be used in the following control design.

In what follows we design the adaptive controller $U(t)$ based on the plant (13)–(18) with the condition that $A_E - \frac{1}{\sqrt{q}}BC_1$ is controllable. This condition is satisfied in the oil drilling model according to (10), (19) and (20).

3. Adaptive update laws for unknown coefficients

The objective in this section is to build adaptive update laws to estimate the unknown coefficients c and a_j, b_j, respectively, where normalization and projection operators are used to guarantee boundedness, as typical in adaptive control designs.

Define adaptive update laws for the unknown coefficient c in the matrix A (10) and the unknown coefficients a_j, b_j in $d(t)$ in (4) as:

$$\dot{\hat{c}}(t) = \gamma_c \text{Proj}_{[0,\bar{c}]}\left(\tau(t), \hat{c}(t)\right), \tag{22}$$

$$\dot{\hat{a}}_j(t) = \gamma_{aj} \text{Proj}_{[0,\bar{a}_j]}\left(\tau_{1j}(t), \hat{a}_j(t)\right), \tag{23}$$

$$\dot{\hat{b}}_j(t) = \gamma_{bj} \text{Proj}_{[0,\bar{b}_j]}\left(\tau_{2j}(t), \hat{b}_j(t)\right), \tag{24}$$

where the positive update gains $\gamma_c, \gamma_{aj}, \gamma_{bj}$ are tuning parameters to be determined. For any $m \le M$ and any r, p, $\text{Proj}_{[m,M]}$ is the standard projection operator (Krstic, 2009a) given by

$$\text{Proj}_{[m,M]}(r,p) = \begin{cases} 0, & \text{if } p = m \text{ and } r < 0, \\ 0, & \text{if } p = M \text{ and } r > 0, \\ r, & \text{else.} \end{cases}$$

The role of the projection operator is to keep the parameter estimates bounded. The bounds $\bar{c}$ and $\bar{a}_j, \bar{b}_j$ are defined in Assumptions 1 and 2 respectively. $\tau, \tau_{1j}, \tau_{2j}$ in (22)–(24) are defined as

$$\tau(t) = \frac{1}{1+\Omega(t)}\Bigg(X^T P A_m - \lambda_a \int_0^L e^x \beta(x,t) \times \left(\bar{\kappa} + \left[0, \frac{\sqrt{q}\hat{c}(t)}{k}\right]\right) e^{\frac{1}{\sqrt{q}}(A_E + \hat{c}(t)A_m - \frac{1}{\sqrt{q}}BC_1)x} A_m dx\Bigg) X(t), \tag{25}$$

$$\tau_{1j}(t) = \frac{1}{k(1+\Omega(t))}\Bigg(X^T P B \cos(\theta_j t) - \lambda_a \int_0^L e^x \beta(x,t) \times \left(\bar{\kappa} + \left[0, \frac{\sqrt{q}\hat{c}(t)}{k}\right]\right) e^{\frac{1}{\sqrt{q}}(A_E + \hat{A}_c(t) - \frac{1}{\sqrt{q}}BC_1)x} B \cos(\theta_j t) dx\Bigg), \tag{26}$$

$$\tau_{2j}(t) = \frac{1}{k(1+\Omega(t))}\Bigg(X^T P B \sin(\theta_j t) - \lambda_a \int_0^L e^x \beta(x,t) \times \left(\bar{\kappa} + \left[0, \frac{\sqrt{q}\hat{c}(t)}{k}\right]\right) e^{\frac{1}{\sqrt{q}}(A_E + \hat{A}_c(t) - \frac{1}{\sqrt{q}}BC_1)x} B \sin(\theta_j t) dx\Bigg). \tag{27}$$

Note that the choices of $\tau(t), \tau_{1j}(t), \tau_{2j}(t)$ will be clear from Lyapunov analysis which will be shown Section 5. The definitions of the parameters and states used in (25)–(27) are shown as follows, i.e., (28)–(39).

$$A_m = \begin{bmatrix} 0 & 0 \\ 0 & \frac{1}{I_b} \end{bmatrix}, \tag{28}$$

$$\hat{A}_c(t) = \begin{bmatrix} 0 & 0 \\ 0 & \frac{\hat{c}(t)}{I_b} \end{bmatrix}, \tag{29}$$

$$\Omega(t) = \frac{1}{2}\lambda_a \int_0^L e^x \beta(x,t)^2 dx + \frac{1}{2}\lambda_b \int_0^L e^{-x} \alpha(x,t)^2 dx + \frac{1}{2} X(t)^T P X(t). \tag{30}$$

Note that normalization $\Omega(t)$ is introduced in the denominator in (25)–(27) to limit the rates of changes of the parameter estimates i,e., $\dot{\hat{c}}(t)$ and $\dot{\hat{a}}_j(t), \dot{\hat{b}}_j(t)$. The normalization constants $\lambda_a > 0, \lambda_b > 0$ are tuning parameters to be determined.

The matrix $P = P^T > 0$, where the superscript T means transposition, is the unique solution to the following Lyapunov equation

$$P\bar{A} + \bar{A}^T P = -Q \tag{31}$$

for some $Q = Q^T > 0$ and $\bar{A} = A_E - \frac{1}{\sqrt{q}}BC_1 + \frac{1}{\sqrt{q}}B\bar{\kappa}$ is made sure to be Hurwitz by appropriately choosing control parameters $\bar{\kappa} = [\bar{k}_1, \bar{k}_2]$ later. $\alpha(x,t), \beta(x,t)$ are defined as

$$\alpha(x,t) = z(x,t) - \frac{\sqrt{q}}{k}[\hat{a}_1(t), \hat{b}_1(t), \ldots, \hat{a}_N(t), \hat{b}_N(t)] e^{-\frac{A_z}{\sqrt{q}}x} Z(t), \tag{32}$$

$$\begin{aligned}\beta(x,t) =& w(x,t) + \frac{\sqrt{q}}{k}[\hat{a}_1(t), \hat{b}_1(t), \ldots, \hat{a}_N(t), \hat{b}_N(t)] e^{\frac{A_z}{\sqrt{q}}x} Z(t) \\ &- \left(\bar{\kappa} + \left[0, \frac{\sqrt{q}\hat{c}(t)}{k}\right]\right) e^{\frac{1}{\sqrt{q}}(A_E + \hat{A}_c(t) - \frac{1}{\sqrt{q}}BC_1)x} X(t) \\ &- \int_0^x \frac{1}{q}\left(\bar{\kappa} + \left[0, \frac{\sqrt{q}\hat{c}(t)}{k}\right]\right) e^{\frac{1}{\sqrt{q}}(A_E + \hat{A}_c(t) - \frac{1}{\sqrt{q}}BC_1)(x-y)} B \\ &\times \Bigg(w(y,t) + \frac{\sqrt{q}}{k}[\hat{a}_1(t), \hat{b}_1(t), \ldots, \hat{a}_N(t), \hat{b}_N(t)] \\ &\times e^{\frac{A_z}{\sqrt{q}}y} Z(t)\Bigg) dy,\end{aligned} \tag{33}$$

where

$$A_z = \text{diag}\left[\begin{pmatrix} 0 & -\theta_1 \\ \theta_1 & 0 \end{pmatrix}, \ldots, \begin{pmatrix} 0 & -\theta_N \\ \theta_N & 0 \end{pmatrix}\right], \tag{34}$$

and

$$Z(t) = [\cos(\theta_1 t), \sin(\theta_1 t), \ldots, \cos(\theta_N t), \sin(\theta_N t)]^T \tag{35}$$

will be used in constructing the transformation in Section 4.1. Note that $\alpha(x,t), \beta(x,t)$ (32)–(33) are derived from transformations (40)–(41) and (60)–(61) which will be shown later. It will be seen clearly in Section 4.

Note that $z(x,t), w(x,t)$ in (32) and (33) can be calculated by the available boundary states through transport PDEs (13)–(17):

$$w(x,t) = w(L, t - \frac{1}{\sqrt{q}}(L-x)), \tag{36}$$

$$z(x,t) = 2C_1 X(t - \frac{1}{\sqrt{q}}x) - w(0, t - \frac{1}{\sqrt{q}}x)$$

$$= 2C_1X(t-\frac{1}{\sqrt{q}}x) - w(L, t-\frac{L}{\sqrt{q}}-\frac{1}{\sqrt{q}}x). \tag{37}$$

Applying (5), (12), (19) then $w(x,t)$, $z(x,t)$ can be written as

$$w(x,t) = u_t\left(L, t-\frac{1}{\sqrt{q}}(L-x)\right) + \sqrt{q}u_x\left(L, t-\frac{1}{\sqrt{q}}(L-x)\right), \tag{38}$$

$$z(x,t) = 2u_t\left(0, t-\frac{1}{\sqrt{q}}x\right) - u_t\left(L, t-\frac{L}{\sqrt{q}}-\frac{1}{\sqrt{q}}x\right) - \sqrt{q}u_x\left(L, t-\frac{L}{\sqrt{q}}-\frac{1}{\sqrt{q}}x\right). \tag{39}$$

Note that $u_t(L, t-\frac{L}{\sqrt{q}}-\frac{1}{\sqrt{q}}x)$, $u_t(L, t-\frac{1}{\sqrt{q}}(L-x))$ are the measurement $u_t(L,t)$ at previous time moments, and recalling (2), $u_x(L, t-\frac{L}{\sqrt{q}}-\frac{1}{\sqrt{q}}x)$ and $u_x(L, t-\frac{1}{\sqrt{q}}(L-x))$ can be replaced by $U(t-\frac{L}{\sqrt{q}}-\frac{1}{\sqrt{q}}x)$ and $U(t-\frac{1}{\sqrt{q}}(L-x))$ which are the control input in the previous time moments as known quantities. Therefore, according to (32)–(35), (38)–(39) and (5), we then have $\alpha(x,t)$, $\beta(x,t)$ and $X(t)$ can be obtained by the available boundary measurements proposed in Section 2.1. Therefore, the adaptive update laws can be determined by the available boundary states proposed in Section 2.1.

4. Output feedback control design

In this section, we would like to design an output feedback controller to compensate the uncertain stick–slip instability and external disturbance at the ODE which is anti-collocated with the controller based on the adaptive laws presented in Section 3, by using the measurements mentioned in Section 2.1. To this end, we first propose a transformation to make the unmatched external disturbance collocated with the controller, and then the disturbance can be more easily canceled via control design.

4.1. Transformation to make control and the unmatched disturbance collocated

We now transform the system (13)–(17) into an intermediate system so that the control input at $x = L$ and the anti-collocated disturbance at the ODE are set to be collocated (Wang, Tang et al., 2018).

We introduce the invertible transformations $(w, z) \to (v, s)$:

$$v(x,t) = w(x,t) + \Gamma(x,t)Z(t), \tag{40}$$

$$s(x,t) = z(x,t) + \Gamma_1(x,t)Z(t), \tag{41}$$

where $\Gamma(x,t)$, $\Gamma_1(x,t)$ are to be determined.

Through (40)–(41), we would like to convert the system (13)–(17) into the following system:

$$\dot{X}(t) = \left(A - \frac{1}{\sqrt{q}}BC_1\right)X(t) + \frac{1}{\sqrt{q}}Bv(0,t) + \frac{1}{k}B\tilde{d}(t), \tag{42}$$

$$s(0,t) + v(0,t) = 2C_1X(t), \tag{43}$$

$$s_t(x,t) = -\sqrt{q}s_x(x,t) + \Gamma_{1t}(x,t)Z(t), \tag{44}$$

$$v_t(x,t) = \sqrt{q}v_x(x,t) + \Gamma_t(x,t)Z(t), \tag{45}$$

$$v(L,t) = 2\sqrt{q}U(t) + s(L,t) + (\Gamma(L,t) - \Gamma_1(L,t))Z(t), \tag{46}$$

where $\tilde{d}(t)$ is defined as

$$\tilde{d}(t) = \sum_{j=1}^{N}\left[\tilde{a}_j(t)\cos(\theta_j t) + \tilde{b}_j(t)\sin(\theta_j t)\right], \tag{47}$$

with $\tilde{a}_j(t)$, $\tilde{b}_j(t)$, $j = 1, \ldots, N$ defined as

$$\tilde{a}_j(t) = a_j - \hat{a}_j(t), \tag{48}$$

$$\tilde{b}_j(t) = b_j - \hat{b}_j(t). \tag{49}$$

Recalling (34)–(35), we immediately have

$$\dot{Z}(t) = A_zZ(t). \tag{50}$$

Taking the time and spatial derivatives of (40) and substituting the result into (45), we get

$$\begin{aligned} &v_t(x,t) - \sqrt{q}v_x(x,t) - \Gamma_t(x,t)Z(t) \\ &= w_t(x,t) - \sqrt{q}w_x(x,t) + \Gamma_t(x,t)Z(t) + \Gamma(x,t)A_zZ(t) \\ &\quad - \sqrt{q}\Gamma_x(x,t)Z(t) - \Gamma_t(x,t)Z(t) \\ &= (\Gamma(x,t)A_z - \sqrt{q}\Gamma_x(x,t))Z(t) = 0. \end{aligned} \tag{51}$$

For (51) to hold, we have the sufficient condition

$$\Gamma(x,t)A_z - \sqrt{q}\Gamma_x(x,t) = 0. \tag{52}$$

By mapping (13) and (42) through the transformation (40), we have the condition

$$\Gamma(0,t) = \frac{\sqrt{q}}{k}[\hat{a}_1(t), \hat{b}_1(t), \ldots, \hat{a}_N(t), \hat{b}_N(t)]. \tag{53}$$

Considering (52)–(53), we obtain the solution

$$\Gamma(x,t) = \frac{\sqrt{q}}{k}[\hat{a}_1(t), \hat{b}_1(t), \ldots, \hat{a}_N(t), \hat{b}_N(t)]e^{\frac{A_z}{\sqrt{q}}x}, \tag{54}$$

where $e^{\frac{A_z}{\sqrt{q}}x}$ can be written as

$$e^{\frac{A_z}{\sqrt{q}}x} = \mathrm{diag}\left[\begin{pmatrix}\cos(\frac{\theta_1}{\sqrt{q}}x), & -\sin(\frac{\theta_1}{\sqrt{q}}x)\\ \sin(\frac{\theta_1}{\sqrt{q}}x), & \cos(\frac{\theta_1}{\sqrt{q}}x)\end{pmatrix}, \ldots, \begin{pmatrix}\cos(\frac{\theta_N}{\sqrt{q}}x), & -\sin(\frac{\theta_N}{\sqrt{q}}x)\\ \sin(\frac{\theta_N}{\sqrt{q}}x), & \cos(\frac{\theta_N}{\sqrt{q}}x)\end{pmatrix}\right], \tag{55}$$

according to (34).

Similarly, mapping (14)–(15) and (43)–(44) through (40)–(41), we obtain

$$\Gamma_1(x,t) = -\frac{\sqrt{q}}{k}[\hat{a}_1(t), \hat{b}_1(t), \ldots, \hat{a}_N(t), \hat{b}_N(t)]e^{-\frac{A_z}{\sqrt{q}}x}. \tag{56}$$

Note that $|\Gamma(x,t)|$ and $|\Gamma_1(x,t)|$ are bounded as

$$\max_{x\in[0,L], t\in[0,\infty)}\{|\Gamma(x,t)|, |\Gamma_1(x,t)|\} \le \frac{\sqrt{2Nq}}{k}\max_{j=1,\ldots,N}\{\bar{a}_j, \bar{b}_j\} \tag{57}$$

where $|\cdot|$ is Euclidean norm, recalling (55) being a rotation matrix and the adaptive estimates $\hat{a}_j(t)$, $\hat{b}_j(t)$ are bounded by $[0, \bar{a}_j]$ and $[0, \bar{b}_j]$ via using the projection operator in Section 3.

Thus, through the transformation (40)–(41) with (54)–(56), we complete the conversion from the plant (13)–(17) to the intermediate system (42)–(46) where the control input and the unmatched disturbance information are collocated.

4.2. Backstepping control design

4.2.1. Backstepping transformation and the target system

In addition to canceling the disturbance term $Z(t)$ at (46) straightforward, the objective in this section is to compensate the uncertain anti-damped term $cu_t(0,t)$ included in (42) by designing the control input $U(t)$ at (46).

The PDE backstepping method (Krstic, 2009c) is used to deign the controller. Recalling (42) and (18), through backstepping transformation, we would like to match the poles of $A_E - \frac{1}{\sqrt{q}}BC_1$ to

form a Hurwitz matrix, and compensate the anti-damping term $A_cX(t)$ by $\hat{A}_c(t)X(t)$. Recalling (21) and (29), we have

$$\tilde{A}_c(t) = A_c - \hat{A}_c(t) = \begin{bmatrix} 0 & 0 \\ 0 & \frac{\tilde{c}(t)}{l_b} \end{bmatrix}, \tag{58}$$

where $\tilde{c}(t)$ is the estimation error of c:

$$\tilde{c}(t) = c - \hat{c}(t). \tag{59}$$

The backstepping transformation is defined as:

$$\alpha(x,t) = s(x,t), \tag{60}$$

$$\beta(x,t) = v(x,t) - \int_0^x \phi(x,y,t)v(y,t)dy - \gamma(x,t)X(t), \tag{61}$$

where the time-varying kernel functions $\phi(x,y,t)$, $\gamma(x,t)$ are to be determined later.

From the spatial causal structure, the inverse transformation of (60)–(61) can be written as

$$s(x,t) = \alpha(x,t), \tag{62}$$

$$v(x,t) = \beta(x,t) - \int_0^x \psi(x,y,t)\beta(y,t)dy - \chi(x,t)X(t), \tag{63}$$

where $\psi(x,y,t)$ and $\chi(x,t)$ are kernel functions to be determined.

Remark 2. The fact that the kernel functions are time-varying in the backstepping transformation (61) is due to adaptive estimation $\hat{c}(t)$ included. Because $\hat{c}(t)$ and $\dot{\hat{c}}(t)$ are bounded according to the designed update laws, $\hat{c}(t)$ is continuous and sufficiently regular.

Through the backstepping transformation (60)–(61) and (62)–(63), we would like to convert the intermediate system (42)–(46) into the following target system:

$$\dot{X}(t) = \bar{A}X(t) + \tilde{A}_c(t)X(t) + \frac{1}{\sqrt{q}}B\beta(0,t) + \frac{1}{k}B\tilde{d}(t), \tag{64}$$

$$\begin{aligned}\beta_t(x,t) = {} & \sqrt{q}\beta_x(x,t) + \Gamma_t(x,t)Z(t) - \int_0^x \phi(x,y,t)\Gamma_t(y,t)dyZ(t) \\ & - (\gamma_t(x,t) + \gamma(x,t)\tilde{A}_c(t))X(t) - \int_0^x \phi_t(x,y,t)\beta(y,t)dy \\ & + \int_0^x \phi_t(x,y,t)\int_0^y \psi(y,\omega,t)\beta(\omega,t)d\omega dy \\ & + \int_0^x \phi_t(x,y,t)\chi(y,t)X(t)dy - \gamma(x,t)\frac{1}{k}B\tilde{d}(t),\end{aligned} \tag{65}$$

$$\alpha_t(x,t) = -\sqrt{q}\alpha_x(x,t) + \Gamma_{1t}(x,t)Z(t), \tag{66}$$

$$\beta(0,t) = -\alpha(0,t) + (\gamma(0,t) + 2C_1)X(t), \tag{67}$$

$$\beta(L,t) = 0, \tag{68}$$

where

$$\bar{A} = A_E - \frac{1}{\sqrt{q}}BC_1 + \frac{1}{\sqrt{q}}B\bar{\kappa} = \frac{k}{\sqrt{q}l_b}\begin{bmatrix} 0 & \frac{\sqrt{q}l_b}{k} \\ -\bar{\kappa}_1 & (1-\bar{\kappa}_2) \end{bmatrix} \tag{69}$$

is Hurwitz by choosing the control parameters $\bar{\kappa}_1, \bar{\kappa}_2$ to satisfy

$$\bar{\kappa}_2 > 1, \quad 0 < \bar{\kappa}_1 < \frac{k(1-\bar{\kappa}_2)^2}{4\sqrt{q}l_b}. \tag{70}$$

4.2.2. Calculating the kernel functions

Taking the time and spatial derivatives of (61) gives

$$\begin{aligned}\beta_t(x,t) = {} & v_t(x,t) - \int_0^x \phi(x,y,t)v_t(y,t)dy \\ & - \int_0^x \phi_t(x,y,t)v(y,t)dy - \gamma(x,t)\dot{X}(t) \\ & - \gamma_t(x,t)X(t).\end{aligned} \tag{71}$$

$$\begin{aligned}\beta_x(x,t) = {} & v_x(x,t) - \int_0^x \phi_x(x,y,t)v(y,t)dy \\ & - \phi(x,x,t)v(x,t) - \gamma_x(x,t)X(t).\end{aligned} \tag{72}$$

According to (42)–(46), the following equality holds

$$\begin{aligned}& \beta_t(x,t) - \sqrt{q}\beta_x(x,t) - \Gamma_t(x,t)Z(t) \\ & + \int_0^x \phi(x,y,t)\Gamma_t(y,t)dyZ(t) + (\gamma_t(x,t) + \gamma(x,t)\tilde{A}_c(t))X(t) \\ & + \int_0^x \phi_t(x,y,t)v(y,t)dy + \gamma(x,t)\frac{1}{k}B\tilde{d}(t) \\ = {} & -\sqrt{q}\int_0^x \phi(x,y,t)v_x(y,t)dy + \sqrt{q}\int_0^x \phi_x(x,y,t)v(y,t)dy \\ & - \gamma(x,t)\dot{X}(t) + \sqrt{q}\gamma_x(x,t)X(t) \\ & + \sqrt{q}\phi(x,x,t)v(x,t) + \gamma(x,t)\tilde{A}_c(t)X(t) + \gamma(x,t)\frac{1}{k}B\tilde{d}(t) \\ = {} & \left(\sqrt{q}\phi(x,0,t) - \frac{1}{\sqrt{q}}\gamma(x,t)B\right)v(0,t) \\ & + \int_0^x \left(\sqrt{q}\phi_x(x,y,t) + \sqrt{q}\phi_y(x,y,t)\right)v(y,t)dy \\ & + \left(\sqrt{q}\gamma_x(x,t) - \gamma(x,t)\left(A_E + \hat{A}_c(t) - \frac{1}{\sqrt{q}}BC_1\right)\right)X(t).\end{aligned} \tag{73}$$

For (73) to be zero, which ensures (65) holds by applying (63), together with mapping (64) with (42) via (61), we have the following kernel conditions:

$$q\phi(x,0,t) = \gamma(x,t)B, \tag{74}$$

$$\phi_x(x,y,t) + \phi_y(x,y,t) = 0, \tag{75}$$

$$\sqrt{q}\gamma_x(x,t) - \gamma(x,t)\left(A_E + \hat{A}_c(t) - \frac{1}{\sqrt{q}}BC_1\right) = 0, \tag{76}$$

$$B\frac{1}{\sqrt{q}}\gamma(0,t) = \frac{1}{\sqrt{q}}B\bar{\kappa} - \hat{A}_c(t). \tag{77}$$

We thus obtain the unique kernel solutions as

$$\gamma(x,t) = \left(\bar{\kappa} + \begin{bmatrix} 0, & \frac{\sqrt{q}\hat{c}(t)}{k} \end{bmatrix}\right) e^{\frac{1}{\sqrt{q}}(A_E + \hat{A}_c(t) - \frac{1}{\sqrt{q}}BC_1)x}, \tag{78}$$

$$\begin{aligned}& \phi(x,y,t) \\ & = \frac{1}{q}\left(\bar{\kappa} + \begin{bmatrix} 0, & \frac{\sqrt{q}\hat{c}(t)}{k} \end{bmatrix}\right) e^{\frac{1}{\sqrt{q}}(A_E + \hat{A}_c(t) - \frac{1}{\sqrt{q}}BC_1)(x-y)}B,\end{aligned} \tag{79}$$

where $\hat{A}_c(t) = -\frac{1}{k}B[0, \hat{c}(t)]$ is used. Note that the adaptive estimation $\hat{c}(t)$ which is continuous and included in the kernel functions (78)–(79) ensures $\gamma(x,t)$ and $\phi(x,y,t)$ are continuous.

Remark 3. The kernels $\psi(x,y,t)$, $\chi(x,t)$ of the inverse transformation (62)–(63) also exist and are continuous. Rewrite (61) as

$$v(x,t) - \int_0^x \phi(x,y,t)v(y,t)dy = \beta(x,t) + \gamma(x,t)X(t).$$

Because $\phi(x,y,t)$ is continuous, recalling Remark 2, it can be concluded that a unique continuous $\eta(x,y,t)$ exists on $\{(x,y)|0 \le y \le x \le L\}$ such that

$$\begin{aligned}v(x,t) = {} & \beta(x,t) + \gamma(x,t)X(t) \\ & + \int_0^x \eta(x,y,t)\left(\beta(y,t) + \gamma(y,t)X(t)\right)dy\end{aligned}$$

$$=\beta(x,t)+\int_0^x \eta(x,y,t)\beta(y,t)dy + \left(\int_0^x \eta(x,y,t)\gamma(y,t)dy+\gamma(x,t)\right)X(t),$$

according to Su, Wang, and Krstic (2018). The kernels in the inverse transformation (62)–(63) are

$$\psi(x,y,t)=-\eta(x,y,t),$$
$$\chi(x,t)=-\int_0^x \eta(x,y,t)\gamma(y,t)dy-\gamma(x,t)$$

which are also continuous recalling the continuity of $\gamma(x,t)$ and $\eta(x,y,t)$.

Note that the two transformations (40)–(41) and (60)–(61) with the kernels (54)–(56) and (78)–(79) determined in Section 4.1 and this section respectively are used to obtain (32) and (33).

4.2.3. Control law

According to the boundary condition (68), (46) and the transformation (61), we can derive the controller as

$$U(t)=\frac{1}{2\sqrt{q}}\Big(-s(L,t)-(\Gamma(L,t)-\Gamma_1(L,t))Z(t) + \int_0^L \phi(L,y,t)v(y,t)dy+\gamma(L,t)X(t)\Big). \tag{80}$$

Using (40)–(41) and (11)–(12), (80) can be rewritten as

$$U(t)=\frac{1}{2\sqrt{q}}\Big(-u_t(L,t)+\sqrt{q}u_x(L,t)-\Gamma(L,t)Z(t) + \int_0^L \phi(L,y,t)\Gamma(y,t)dyZ(t)+\gamma(L,t)X(t) + \int_0^L \phi(L,y,t)\Big[u_t\left(L,t-\frac{1}{\sqrt{q}}(L-y)\right) + \sqrt{q}u_x\left(L,t-\frac{1}{\sqrt{q}}(L-y)\right)\Big]dy\Big), \tag{81}$$

where

$$v(y,t)=w\left(L,t-\frac{1}{\sqrt{q}}(L-y)\right)+\Gamma(y,t)Z(t) \tag{82}$$

is used, which is obtained by (38), (40).

Substituting (54)–(56), (78)–(79) and (5), the controller (81) can be written as

$$\begin{aligned}U(t)=&\frac{1}{2\sqrt{q}}\Big[-u_t(L,t)+\sqrt{q}u_x(L,t)\\ &-\frac{\sqrt{q}}{k}[\hat{a}_1(t),\hat{b}_1(t),\ldots,\hat{a}_N(t),\hat{b}_N(t)]e^{\frac{A_Z}{\sqrt{q}}L}Z(t)\\ &+\frac{1}{q}\left(\bar{\kappa}+\left[0,\frac{\sqrt{q}\hat{c}(t)}{k}\right]\right)\int_0^L e^{\frac{1}{\sqrt{q}}(A_E+\hat{c}(t)A_m-\frac{1}{\sqrt{q}}BC_1)(L-y)}B\\ &\times\frac{\sqrt{q}}{k}[\hat{a}_1(t),\hat{b}_1(t),\ldots,\hat{a}_N(t),\hat{b}_N(t)]e^{\frac{A_Z}{\sqrt{q}}y}dyZ(t)\\ &+\left(\bar{\kappa}+\left[0,\frac{\sqrt{q}\hat{c}(t)}{k}\right]\right)e^{\frac{1}{\sqrt{q}}(A_E+\hat{c}(t)A_m-\frac{1}{\sqrt{q}}BC_1)L}\\ &\times[u(0,t),u_t(0,t)]^T+\frac{1}{q}\left(\bar{\kappa}+\left[0,\frac{\sqrt{q}\hat{c}(t)}{k}\right]\right)\\ &\times\int_{t-\frac{L}{\sqrt{q}}}^t e^{(A_E+\hat{c}(t)A_m-\frac{1}{\sqrt{q}}BC_1)(t-\delta)}B\\ &\times[u_t(L,\delta)+\sqrt{q}u_x(L,\delta)]d\delta\Big],\end{aligned} \tag{83}$$

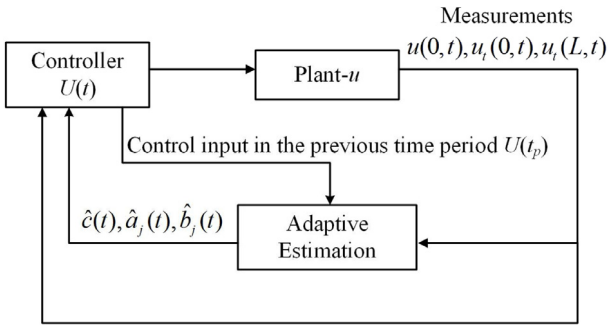

Fig. 2. The block diagram of the closed-loop system.

where $\hat{A}_c(t)=\hat{c}(t)A_m$ ensured by (28) and (29) is used. $Z(t)$ is defined as (35) and $\hat{c}(t)$, $\hat{a}_j(t)$, $\hat{b}_j(t)$, $j=1,\ldots,N$ are calculated from the adaptive update laws (22) and (25), (23) and (26), (24) and (27) proposed in Section 3. $u(0,t)$, $u_t(0,t)$, $u_t(L,t)$ are obtained from measurements in Section 2.1. $u_x(L,t)$ can be replaced as $U(t)$ by applying (2), and the refreshed control input is shown in the following paragraph.

We choose the controller to be activated at $t=\frac{2L}{\sqrt{q}}$ to make sure the second argument of $w(L,t-\frac{L}{\sqrt{q}}-\frac{x}{\sqrt{q}})$ in (37) is positive. In other words, the system runs as open-loop and $U(t)=0$ when $t\in[0,\frac{2L}{\sqrt{q}})$. Substituting (2) into (83) to replace $u_x(L,t)$ as $U(t)$, the control input can be rewritten as

$$\begin{aligned}U(t)=&\frac{1}{\sqrt{q}}\Big[-u_t(L,t)-\frac{\sqrt{q}}{k}[\hat{a}_1(t),\hat{b}_1(t),\ldots,\hat{a}_N(t),\hat{b}_N(t)]e^{\frac{A_Z}{\sqrt{q}}L}Z(t)\\ &+\frac{1}{q}\left(\bar{\kappa}+\left[0,\frac{\sqrt{q}\hat{c}(t)}{k}\right]\right)\int_0^L e^{\frac{1}{\sqrt{q}}(A_E+\hat{c}(t)A_m-\frac{1}{\sqrt{q}}BC_1)(L-y)}B\\ &\times\frac{\sqrt{q}}{k}[\hat{a}_1(t),\hat{b}_1(t),\ldots,\hat{a}_N(t),\hat{b}_N(t)]e^{\frac{A_Z}{\sqrt{q}}y}dyZ(t)\\ &+\left(\bar{\kappa}+\left[0,\frac{\sqrt{q}\hat{c}(t)}{k}\right]\right)e^{\frac{1}{\sqrt{q}}(A_E+\hat{c}(t)A_m-\frac{1}{\sqrt{q}}BC_1)L}\\ &\times[u(0,t),u_t(0,t)]^T\\ &+\frac{1}{q}\left(\bar{\kappa}+\left[0,\frac{\sqrt{q}\hat{c}(t)}{k}\right]\right)\int_{t-\frac{L}{\sqrt{q}}}^t e^{(A_E+\hat{c}(t)A_m-\frac{1}{\sqrt{q}}BC_1)(t-\delta)}B\\ &\times[u_t(L,\delta)+\sqrt{q}U(\delta)]d\delta\Big],\quad t\geq\frac{2L}{\sqrt{q}},\end{aligned} \tag{84}$$

where the value $U(\delta)$ of the control input in the previous time interval $\delta\in[t-\frac{L}{\sqrt{q}},t)$ would be used. Note that $U(\bar{\delta}_1)$ with $\bar{\delta}_1\in[t-\frac{2L}{\sqrt{q}},t)$ will also be used according to (30), (32)–(33) and (38)–(39) in building the estimation of $\hat{c}(t)$, $\hat{a}_j(t)$, $\hat{b}_j(t)$. Because $U(t)$ in the previous time interval $t\in[0,\frac{2L}{\sqrt{q}})$ is zero, therefore $U(\delta)$, $U(\bar{\delta}_1)$ can be regarded as known quantities in calculating $U(t)$ (84) at $t=\frac{2L}{\sqrt{q}}$. By that analogy, $U(t)$ at each time point in $t\geq\frac{2L}{\sqrt{q}}$ can be calculated by the measurements $u(0,t)$, $u_t(0,t)$, $u_t(L,t)$ and $U(\delta)$, $U(\bar{\delta}_1)$ in the previous steps. Therefore, the proposed output feedback controller (84) is entirely computable with the available boundary measurements $u(0,t)$, $u_t(0,t)$, $u_t(L,t)$. The block diagram of the closed-loop system is shown in Fig. 2.

5. Stability analysis

5.1. Stability analysis of (42)–(46)

Before proving the main result of this paper, we propose the following lemma.

Lemma 1. *If the initial data $s(\cdot,0)$, $v(\cdot,0)$ both belong to $L^2(0,L)$, then the system (42)–(46) under the control (80) is well-posed, and it is uniformly bounded and asymptotically stable in the sense of the norm*

$$\left(\|s(\cdot,t)\|^2+\|v(\cdot,t)\|^2+|X(t)|^2\right)^{1/2}. \tag{85}$$

Proof of Lemma 1. The well-posedness of the closed-loop system-(s,v) can be obtained if the well-posedness of the target system-(α,β) (64)–(68) is achieved, because the backstepping transformation (60)–(61) is continuous and invertible. Because the adaptive estimate laws $\hat{c}(t)$, $\hat{a}_j(t)$, $\hat{b}_j(t)$ for the unknown constant coefficients c, a_j, b_j which are constants are determined by some normal ODEs, it is obvious that the estimation errors $\tilde{c}(t)$, $\tilde{a}_j(t)$, $\tilde{b}_j(t)$ are well defined. The well-posedness of the target system (64)–(68) in the non-adaptive case, i.e., $\tilde{A}_c(t)=0$, $\tilde{d}(t)=0$ can be proved similar to Di Meglio, Bribiesca, Hu, and Krstic (2018). Considering $Z(t)$ defined as (35) and $\tilde{A}_c(t)$, $\tilde{d}(t)$ defined as (58), (47) being some well-defined injections of (64)–(68), the well-posedness of the closed-loop system-(s,v) can then be proved.

Define

$$\Theta(t)=\|\beta(\cdot,t)\|^2+\|\alpha(\cdot,t)\|^2+|X(t)|^2, \tag{86}$$

where $\|\cdot\|$ denotes the L_2 norm. Recalling (30), we have

$$\mu_1\Theta(t)\le\Omega(t)\le\mu_2\Theta(t), \tag{87}$$

with positive μ_1,μ_2 as

$$\mu_1=\frac{1}{2}\min\{\lambda_a,\lambda_b e^{-L},\lambda_{\min}(P)\}, \tag{88}$$

$$\mu_2=\frac{1}{2}\min\{\lambda_a e^{L},\lambda_b,\lambda_{\max}(P)\}, \tag{89}$$

where $\lambda_{\min}$ and $\lambda_{\max}$ denote the minimum and maximum eigenvalues of the corresponding matrix.

Choose a Lyapunov function as

$$V(t)=\ln(1+\Omega(t))+\sum_{j=1}^{N}\frac{1}{2\gamma_{aj}}\tilde{a}_j(t)^2+\sum_{j=1}^{N}\frac{1}{2\gamma_{bj}}\tilde{b}_j(t)^2+\frac{1}{2\gamma_c}\tilde{c}(t)^2, \tag{90}$$

where $\tilde{a}_j(t)$, $\tilde{b}_j(t)$, $\tilde{c}(t)$ are defined in (48)–(49) and (59) respectively.

Considering (87) and the monotone increasing function $\ln(\cdot)$, the following inequality holds

$$\begin{aligned}0\le{}&\ln(1+\mu_1\Theta(t))+\bar{\mu}_1\left(\sum_{j=1}^{N}\left(\tilde{a}_j(t)^2+\tilde{b}_j(t)^2\right)+\tilde{c}(t)^2\right)\\ &\le V(t)\le\ln(1+\mu_2\Theta(t))\\ &\quad+\bar{\mu}_2\left(\sum_{j=1}^{N}\left(\tilde{a}_j(t)^2+\tilde{b}_j(t)^2\right)+\tilde{c}(t)^2\right),\end{aligned} \tag{91}$$

where

$$\bar{\mu}_1=\frac{1}{2\max_{j\in\{1\cdots N\}}\{\gamma_{aj},\gamma_{bj},\gamma_c\}}>0,$$

$$\bar{\mu}_2=\frac{1}{2\min_{j\in\{1\cdots N\}}\{\gamma_{aj},\gamma_{bj},\gamma_c\}}>0. \tag{92}$$

Taking the derivative of (90) and inserting (64), we have

$$\begin{aligned}\dot{V}(t)=\frac{1}{1+\Omega(t)}\Bigg(&-X(t)^TQX(t)+\frac{1}{\sqrt{q}}X^TPB\beta(0,t)\\ &+X^TP\frac{B}{k}\sum_{j=1}^{N}[\tilde{a}_j(t)\cos(\theta_j t)+\tilde{b}_j(t)\sin(\theta_j t)]\\ &+X^TP\tilde{c}(t)A_mX(t)+\lambda_a\int_0^L e^x\beta(x,t)\beta_t(x,t)dx\\ &+\lambda_b\int_0^L e^{-x}\alpha(x,t)\alpha_t(x,t)dx\Bigg)-\sum_{j=1}^{N}\frac{1}{\gamma_{aj}}\dot{\hat{a}}_j(t)\tilde{a}_j(t)\\ &-\sum_{j=1}^{N}\frac{1}{\gamma_{bj}}\dot{\hat{b}}_j(t)\tilde{b}_j(t)-\frac{1}{\gamma_c}\dot{\hat{c}}(t)\tilde{c}(t),\end{aligned} \tag{93}$$

where $\tilde{A}(t)=\tilde{c}(t)A_m$ ensured by (28) and (58) is used.

Inserting (65)–(68) into (93) and applying Cauchy–Schwarz inequality, we obtain

$$\begin{aligned}\dot{V}(t)\le{}&\frac{1}{1+\Omega(t)}\Bigg[-\left(\frac{3}{4}\lambda_{\min}(Q)-\sqrt{q}\lambda_b(\gamma(0,t)+2C_1)^2\right)|X(t)|^2\\ &-\frac{1}{2}\sqrt{q}\lambda_a\int_0^L e^x\beta(x,t)^2dx-\lambda_a\int_0^L e^x\beta(x,t)\gamma_t(x,t)dxX(t)\\ &-\lambda_a\int_0^L e^x\beta(x,t)\Bigg(\int_0^x\phi_t(x,y,t)\beta(y,t)dy\\ &-\int_0^x\phi_t(x,y,t)\int_0^y\psi(y,\omega,t)\beta(\omega,t)d\omega dy\\ &-\int_0^x\phi_t(x,y,t)\chi(y,t)X(t)dy\Bigg)dx-\frac{1}{2}\sqrt{q}\lambda_b e^{-L}\alpha(L,t)^2\\ &-\left(\frac{1}{2}\sqrt{q}\lambda_a-\frac{|PB|^2}{q\lambda_{\min}(Q)}-\sqrt{q}\lambda_b\right)\beta(0,t)^2\\ &-\frac{1}{2}\sqrt{q}\lambda_b\int_0^L e^{-x}\alpha(x,t)^2dx+\lambda_b\int_0^L e^{-x}\alpha(x,t)\Gamma_{1t}(x,t)Z(t)dx\\ &+\lambda_a\int_0^L e^x\beta(x,t)\Gamma_t(x,t)Z(t)dx\\ &-\lambda_a\int_0^L e^x\beta(x,t)\int_0^x\phi(x,y,t)\Gamma_t(y,t)dyZ(t)dx\Bigg]\\ &+\sum_{j=1}^{N}\Bigg(\frac{X^TPB\cos(\theta_j t)}{k(1+\Omega(t))}\\ &-\frac{\lambda_a\int_0^L e^x\beta(x,t)\gamma(x,t)B\cos(\theta_j t)dx}{k(1+\Omega(t))}-\frac{1}{\gamma_a}\dot{\hat{a}}_j(t)\Bigg)\tilde{a}_j(t)\\ &+\sum_{j=1}^{N}\Bigg(\frac{X^TPB\sin(\theta_j t)}{k(1+\Omega(t))}\\ &-\frac{\lambda_a\int_0^L e^x\beta(x,t)\gamma(x,t)B\sin(\theta_j t)dx}{k(1+\Omega(t))}-\frac{1}{\gamma_b}\dot{\hat{b}}_j(t)\Bigg)\tilde{b}_j(t)\\ &+\Bigg(\frac{X^TPA_mX(t)}{1+\Omega(t)}\\ &-\frac{\lambda_a\int_0^L e^x\beta(x,t)\gamma(x,t)A_mdxX(t)}{1+\Omega(t)}-\frac{1}{\gamma_c}\dot{\hat{c}}(t)\Bigg)\tilde{c}(t).\end{aligned} \tag{94}$$

Step 1. Consider the third and fourth terms in the square bracket in (94).

Because $\hat{c}(t)\in[0,\bar{c}]$, one can see that $\gamma(x,t)$, $\phi(x,y,t)$ are bounded according to (78)–(79). Here we define

$$\bar{\gamma}=\max\{|\gamma(x,t)|;x\in[0,L],t\in[0,\infty)\}, \tag{95}$$

$$\bar{\phi}=\max\{|\phi(x,y,t)|;x\in[0,L],y\in[0,L],t\in[0,\infty)\}. \tag{96}$$

Similarly, the boundedness of $\chi(x,t)$, $\psi(x,y,t)$ also can be obtained, defining

$$\bar{\chi} = \max\{|\chi(x,t)|; x \in [0,L], t \in [0,\infty)\}, \tag{97}$$

$$\bar{\psi} = \max\{|\psi(x,y,t)|; x \in [0,L], y \in [0,L], t \in [0,\infty)\}. \tag{98}$$

Applying Cauchy–Schwarz inequality and Young's inequality into the numerator of (25), we straightforwardly have the absolute value of the numerator is less than or equal to $m_1(|X(t)|^2 + \|\beta(\cdot,t)\|^2)$ for some positive m_1. Recalling $\Omega(t)$ (30) in the denominator of (25), we also have

$$1+\Omega(t) > \frac{1}{2}\min\{\lambda_a, \lambda_b e^{-L}, \lambda_{\min}(P)\}(|X(t)|^2 + \|\beta(\cdot,t)\|^2).$$

It follows that

$$\begin{aligned}\left|\dot{\hat{c}}(t)\right| \le& \frac{2\gamma_c m_1(|X(t)|^2 + \|\beta(\cdot,t)\|^2)}{\min\{\lambda_a, \lambda_b e^{-L}, \lambda_{\min}(P)\}(|X(t)|^2 + \|\beta(\cdot,t)\|^2)}\\ =& \frac{2\gamma_c m_1}{\min\{\lambda_a, \lambda_b e^{-L}, \lambda_{\min}(P)\}}\end{aligned} \tag{99}$$

via (22).

Recalling (78)–(79), we obtain the boundedness of $\gamma_t(x,t)$ and $\phi_t(x,t)$ as

$$\begin{aligned}|\gamma_t(x,t)| =& \left|\left[0, \frac{\sqrt{q}\dot{\hat{c}}(t)}{k}\right] + \left(\bar{\kappa} + \left[0, \frac{\sqrt{q}\hat{c}(t)}{k}\right]\right)\frac{\dot{\hat{c}}(t)}{\sqrt{q}}A_m\right| m_e\\ \le& \frac{\gamma_c m_c m_e}{\min\{\lambda_a, \lambda_b e^{-L}, \lambda_{\min}(P)\}},\end{aligned} \tag{100}$$

$$|\phi_t(x,t)| \le \frac{\gamma_c m_c m_e |B|}{q\min\{\lambda_a, \lambda_b e^{-L}, \lambda_{\min}(P)\}}, \tag{101}$$

where the constants m_c, m_e are

$$m_c = \frac{2\sqrt{q}m_1}{k} + \frac{2}{l_b\sqrt{q}}\sqrt{|\bar{\kappa}|^2 + \frac{q\bar{c}^2}{k^2}}m_1, \tag{102}$$

$$m_e = \max_{\hat{c}(t)\in[0,\bar{c}], x\in[0,L]}\left\{\bar{\sigma}\left(e^{\frac{1}{\sqrt{q}}(A_E+\hat{c}(t)A_m-\frac{1}{\sqrt{q}}BC_1)x}\right)\right\}. \tag{103}$$

Note that $\bar{\sigma}\left(e^{\frac{1}{\sqrt{q}}(A_E+\hat{c}(t)A_m-\frac{1}{\sqrt{q}}BC_1)x}\right)$ in (103) stands for the largest singular value of $e^{\frac{1}{\sqrt{q}}(A_E+\hat{c}(t)A_m-\frac{1}{\sqrt{q}}BC_1)x}$ at $c(t)$ and x.

Applying Young's and Cauchy–Schwarz inequalities into the third and fourth terms in the square bracket in (94), using (97)–(101), we have

$$\begin{aligned}&\lambda_a\int_0^L e^x\beta(x,t)\gamma_t(x,t)dx X(t)\\ \le& \frac{\gamma_c\bar{M}_0}{\min\{\lambda_a, \lambda_b e^{-L}, \lambda_{\min}(P)\}}\left(\|\beta(\cdot,t)\|^2 + |X(t)|^2\right),\end{aligned} \tag{104}$$

$$\begin{aligned}&\lambda_a\int_0^L e^x\beta(x,t)\left(\int_0^x \phi_t(x,y,t)\beta(y,t)dy\right.\\ &-\int_0^x \phi_t(x,y,t)\int_0^y \psi(y,\omega,t)\beta(\omega,t)d\omega dy\\ &\left.-\int_0^x \phi_t(x,y,t)\chi(y,t)X(t)dy\right)dx\\ \le& \frac{\gamma_c\bar{M}_1}{\min\{\lambda_a, \lambda_b e^{-L}, \lambda_{\min}(P)\}}\left(\|\beta(\cdot,t)\|^2 + |X(t)|^2\right),\end{aligned} \tag{105}$$

where

$$\bar{M}_0 = 2\lambda_a e^L m_c m_e \max\{L,1\},$$

$$\bar{M}_1 = \lambda_a e^L L\frac{1}{q}m_c m_e|B|\max\{1+L\bar{\psi}+2\bar{\chi}, 2\bar{\chi}L\}.$$

Step 2. Consider the eighth to tenth terms in the square bracket in (94).

Applying Cauchy–Schwarz inequality and Young's inequality into the numerator of (26)–(27), together with $1+\Omega(t) \ge 1$ in the denominator, we straightforwardly have $\max_{j=1,\dots,N}\{\tau_{1j}(t), \tau_{2j}(t)\} \le m_2\left(|X(t)| + \sqrt{L}\|\beta(\cdot,t)\|\right)$ for any t, where $m_2 = \max\{4|PB|, 2e^L\lambda_a\sqrt{L}\bar{\gamma}|B|\} > 0$. Therefore, we have

$$\begin{aligned}&\max_{j=1,\dots,N}\left\{\left|\dot{\hat{a}}_j(t)\right|, \left|\dot{\hat{b}}_j(t)\right|\right\}\\ \le& m_2\max_{j=1,\dots,N}\{\gamma_{aj}, \gamma_{bj}\}\left(|X(t)| + \sqrt{L}\|\beta(\cdot,t)\|\right)\end{aligned} \tag{106}$$

regarding (23)–(24).

According to (54)–(56), one obtains

$$\begin{aligned}&\max_{x\in[0,L],t\in[0,\infty)}\{|\Gamma_t(x,t)|, |\Gamma_{1t}(x,t)|\}\\ \le& \frac{\sqrt{q}}{k}\left|\dot{\hat{a}}_1(t), \dot{\hat{b}}_1(t), \dots, \dot{\hat{a}}_N(t), \dot{\hat{b}}_N(t)\right|\\ \le& \frac{\sqrt{2qN}}{k}m_2\max_{j=1,\dots,N}\{\gamma_{aj}, \gamma_{bj}\}\left(|X(t)| + \sqrt{L}\|\beta(\cdot,t)\|\right).\end{aligned} \tag{107}$$

Recalling (107), applying Young's inequality into the eighth to tenth terms in the square bracket in (94), we have

$$\begin{aligned}&\lambda_b\int_0^L e^{-x}\alpha(x,t)\Gamma_{1t}(x,t)Z(t)dx\\ \le& \max_{j=1,\dots,N}\{\gamma_{aj}, \gamma_{bj}\}\bar{M}_2\left(\|\alpha(\cdot,t)\|^2 + \|\beta(\cdot,t)\|^2 + |X(t)|^2\right),\end{aligned} \tag{108}$$

$$\begin{aligned}&\lambda_a\int_0^L e^x\beta(x,t)\Gamma_t(x,t)Z(t)dx\\ &-\lambda_a\int_0^L e^x\beta(x,t)\int_0^x \phi(x,y,t)\Gamma_t(y,t)dyZ(t)dx\\ \le& \max_{j=1,\dots,N}\{\gamma_{aj}, \gamma_{bj}\}\bar{M}_3\left(\|\beta(\cdot,t)\|^2 + |X(t)|^2\right),\end{aligned} \tag{109}$$

for some positive constants $\bar{M}_2$, $\bar{M}_3$, where $|Z(t)| = \sqrt{N}$ and (96) are used.

Step 3. Substituting (104)–(105), (108)–(109), (22)–(24), (78) into (94), applying again Young's inequality, we have

$$\begin{aligned}\dot{V}(t) \le& \frac{1}{1+\Omega(t)}\left(-h_1|X(t)|^2 - h_2\|\beta(\cdot,t)\|^2\right.\\ &\left.-h_3\|\alpha(\cdot,t)\|^2 - h_4\alpha(L,t)^2 - h_5\beta(0,t)^2\right),\end{aligned}$$

where

$$\begin{aligned}h_1 =& \frac{3}{4}\lambda_{\min}(Q) - \sqrt{q}\lambda_b(\gamma(0,t)+2C_1)^2\\ &-\frac{\gamma_c\bar{M}_0 + \gamma_c\bar{M}_1}{\min\{\lambda_a, \lambda_b e^{-L}, \lambda_{\min}(P)\}}\\ &-\max_{j=1,\dots,N}\{\gamma_{aj}, \gamma_{bj}\}(\bar{M}_2 + \bar{M}_3),\\ h_2 =& \frac{1}{2}\sqrt{q}\lambda_a - \frac{\gamma_c\bar{M}_0 + \gamma_c\bar{M}_1}{\min\{\lambda_a, \lambda_b e^{-L}, \lambda_{\min}(P)\}}\\ &-\max_{j=1,\dots,N}\{\gamma_{aj}, \gamma_{bj}\}(\bar{M}_2 + \bar{M}_3),\\ h_3 =& \frac{1}{2}\sqrt{q}\lambda_b e^{-L} - \max_{j=1,\dots,N}\{\gamma_{aj}, \gamma_{bj}\}\bar{M}_2,\\ h_4 =& \frac{1}{2}\sqrt{q}\lambda_b e^{-L} > 0,\\ h_5 =& \frac{1}{2}\sqrt{q}\lambda_a - \frac{|PB|^2}{q\lambda_{\min}(Q)} - \sqrt{q}\lambda_b.\end{aligned}$$

Choosing $\lambda_a > \frac{2|PB|^2}{q\sqrt{q}\lambda_{\min}(Q)} + 2\lambda_b$ to guarantee $h_5 > 0$, and using sufficiently small positive constants $\lambda_b, \gamma_{aj}, \gamma_{bj}, \gamma_c$ to make $h_1 > 0$, $h_2 > 0$ and $h_3 > 0$, we obtain

$$\dot{V}(t) \leq \frac{-\xi}{1+\Omega(t)}\Big(|X(t)|^2 + \|\beta(\cdot,t)\|^2 + \|\alpha(\cdot,t)\|^2 + \alpha(L,t)^2 + \beta(0,t)^2\Big) \tag{110}$$

with a positive $\xi = \min\{h_1, h_2, h_3, h_4, h_5\}$, and hence

$$V(t) \leq V(0), \quad \forall t \geq 0. \tag{111}$$

Step 4. Recalling (91), one easily get that $\tilde{c}(t)$, $\tilde{a}_j(t)$, $\tilde{b}_j(t)$, $j = 1, \ldots, N$ and $\Theta(t)$ are uniformly bounded. Therefore, together with (86), we obtain that $\|\beta(\cdot,t)\|$, $\|\alpha(\cdot,t)\|$, $|X(t)|$ are uniformly bounded. It follows that $\|v(\cdot,t)\|$, $\|s(\cdot,t)\|$ are uniformly bounded via (62)–(63). By recalling (47) and (58), we also have $\tilde{d}(t)$, $|\tilde{A}_c(t)|$ are uniformly bounded. According to (107), we have $\Gamma_t(x,t)$ and $\Gamma_{1t}(x,t)$ are bounded.

According to (64)–(68), we further have

$$\frac{d}{dt}|X(t)|^2 = 2X^T(t)\Big(\bar{A}X(t) + \tilde{A}_c(t)X(t) + B\frac{1}{\sqrt{q}}\beta(0,t) + B\frac{1}{k}\tilde{d}(t)\Big), \tag{112}$$

$$\begin{aligned}\frac{d}{dt}\|\beta(\cdot,t)\|^2 =& -\sqrt{q}\beta(0,t)^2 + 2\int_0^L \beta(x,t)\Big(\Gamma_t(x,t)Z(t) \\ &- \int_0^x \phi(x,y,t)\Gamma_t(y,t)dyZ(t) \\ &- (\gamma_t(x,t) + \gamma(x,t)\tilde{A}_c(t))X(t) \\ &- \int_0^x \phi_t(x,y,t)\beta(y,t)dy \\ &+ \int_0^x \phi_t(x,y,t)\int_0^y \psi(y,\omega,t)\beta(\omega,t)d\omega dy \\ &+ \int_0^x \phi_t(x,y,t)\chi(y,t)X(t)dy \\ &- \gamma(x,t)\frac{B}{k}\tilde{d}(t)\Big)dx,\end{aligned} \tag{113}$$

$$\begin{aligned}\frac{d}{dt}\|\alpha(\cdot,t)\|^2 =& -\sqrt{q}\alpha(L,t)^2 + \sqrt{q}\alpha(0,t)^2 \\ &+ 2\int_0^L \alpha(x,t)\Gamma_{1t}(x,t)Z(t)dx.\end{aligned} \tag{114}$$

Recalling (61) and (68), we have $v(L,t)$ is uniformly bounded. According to (40) and the boundedness of $\Gamma(x,t)$, we obtain $w(L,t)$ is uniformly bounded. Because $w(0,t) = w(L, t - \frac{L}{\sqrt{q}})$, $w(0,t)$ is uniformly bounded for $t > \frac{L}{\sqrt{q}}$. Therefore, $z(0,t)$ is uniformly bounded via (14). Because $z(L,t) = z(0, t - \frac{L}{\sqrt{q}})$, $z(L,t)$ is uniformly bounded for $t > \frac{L}{\sqrt{q}}$. According to (40)–(41) together with the boundedness of $\Gamma(x,t)$, $\Gamma_1(x,t)$, and (60)–(61), we have $\beta(0,t)$, $\beta(L,t)$, $\alpha(L,t)$, $\alpha(0,t)$ are uniformly bounded.

Applying Cauchy–Schwarz inequality, we obtain

$$\frac{d}{dt}|X(t)|^2 \leq \mu_3\left(|X(t)|^2 + \beta(0,t)^2 + \tilde{d}(t)^2\right),$$

$$\frac{d}{dt}\|\beta(\cdot,t)\|^2 \leq \mu_4\left(\|\beta(\cdot,t)\|^2 + |X(t)|^2 + \beta(0,t)^2 + \tilde{d}(t)^2\right),$$

$$\frac{d}{dt}\|\alpha(\cdot,t)\|^2 \leq \mu_5\Big(\|\alpha(\cdot,t)\|^2 + \|\beta(\cdot,t)\|^2 + |X(t)|^2 + \alpha(0,t)^2 + \alpha(L,t)^2\Big),$$

with some positive constants μ_3, μ_4, μ_5. Thus $\frac{d}{dt}|X(t)|^2$, $\frac{d}{dt}\|\beta(\cdot,t)\|^2$ and $\frac{d}{dt}\|\alpha(\cdot,t)\|^2$ are uniformly bounded recalling the above boundedness results.

Finally, integrating (110) from 0 to ∞, it follows that $|X(t)|$, $\|\alpha(\cdot,t)\|$, $\|\beta(\cdot,t)\|$ are square integrable. Following Barbalat's Lemma that $|X(t)|$, $\|\alpha(\cdot,t)\|$, $\|\beta(\cdot,t)\|$ tend to zero as $t \to \infty$.

Considering the invertibility and continuity of the backstepping transformations (60)–(61) and (62)–(63), the proof of Lemma 1 is completed.

5.2. Stability analysis of the closed-loop system

The closed-loop system is

$$u_{tt}(x,t) = qu_{xx}(x,t), \tag{115}$$

$$u_x(L,t) = U(t), \tag{116}$$

$$I_b u_{tt}(0,t) = cu_t(0,t) - ku_x(0,t) - d(t), \tag{117}$$

$$d(t) = \sum_{j=1}^{N}[a_j\cos(\theta_j t) + b_j\sin(\theta_j t)], \tag{118}$$

$$\dot{\hat{c}}(t) = \gamma_c \mathrm{Proj}_{[0,\bar{c}]}\{\tau(t), \hat{c}(t)\}, \tag{119}$$

$$\dot{\hat{a}}_j(t) = \gamma_{aj}\mathrm{Proj}_{[0,\bar{a}_j]}\{\tau_{1j}(t), \hat{a}_j(t)\}, \tag{120}$$

$$\dot{\hat{b}}_j(t) = \gamma_{bj}\mathrm{Proj}_{[0,\bar{b}_j]}\{\tau_{2j}(t), \hat{b}_j(t)\}, \tag{121}$$

where the control input $U(t)$ is defined in (84). Note that $\tau(t)$, $\tau_{1j}(t)$, $\tau_{2j}(t)$ which are defined in (25)–(27) can be represented as the original state u by applying (32)–(35), (38)–(39) and (5).

Define $\mathcal{H} = H^2(0,L) \times H^1(0,L)$, where

$$H^1(0,L) = \{u | u(\cdot,t) \in L^2(0,L), u_x(\cdot,t) \in L^2(0,L)\},$$

$$H^2(0,L) = \{u | u(\cdot,t) \in L^2(0,L), u_x(\cdot,t) \in L^2(0,L), u_{xx}(\cdot,t) \in L^2(0,L)\}$$

and $u(\cdot,t) \in L^2(0,L)$ denotes $u(\cdot,t)$ is square integrable. The main result is presented in the following theorem.

Theorem 1. *For any initial values $(u(\cdot,0), u_t(\cdot,0)) \in \mathcal{H}$, the closed-loop system including the plant (115)–(117) and the controller (84) with the adaptive update laws (119)–(121) has the following properties:*

(1) The closed-loop system is well-posed.

(2) The outputs $u(0,t), u_t(0,t)$ of the closed-loop system are asymptotically convergent to the origin in the sense that

$$\lim_{t\to\infty} u(0,t) = 0, \quad \lim_{t\to\infty} u_t(0,t) = 0.$$

(3) Distributed states in the closed-loop system are ultimately uniformly bounded in the sense of the norm

$$\left(\|u_x(\cdot,t)\|^2 + \|u_t(\cdot,t)\|^2\right)^{\frac{1}{2}}.$$

Proof of Theorem 1. Recalling the well-posedness of the closed-loop system-(s,v) proved in Lemma 1 and the invertible transformations $(s,v \longleftrightarrow z,w)$ (40)–(41), $(z,w \longleftrightarrow u)$ (11)–(12), considering $Z(t)$ is well defined as (35), the property 1 of Theorem 1 can then be proved.

According to the asymptotic stability result in Lemma 1, we know that $X(t) = [u(0,t), u_t(0,t)]^T$ is asymptotically convergent to zero, and thus the property 2 of Theorem 1 is proved.

Recalling (40)–(41) and applying Cauchy–Schwarz inequality, we obtain

$$\|w(\cdot,t)\|^2 \leq 2\|v(\cdot,t)\|^2 + 2N\|\Gamma(\cdot,t)\|^2, \tag{122}$$

$$\|z(x,t)\|^2 \le 2\|s(\cdot,t)\|^2 + 2N\|\Gamma_1(\cdot,t)\|^2, \tag{123}$$

where $Z(t)^2 = N$ is used. $\|\Gamma(\cdot,t)\|^2$, $\|\Gamma_1(\cdot,t)\|^2$ are bounded by a positive constant considering (57). Together with convergence to zero and uniform boundedness of $\|v(\cdot,t)\|^2 + \|s(\cdot,t)\|^2$ proved in Lemma 1, we obtain uniform ultimate boundedness of $\|w(\cdot,t)\|^2$, $\|z(\cdot,t)\|^2$. Recalling (11) and (12), we have

$$u_t(x,t) = \frac{1}{2}(z(x,t) + w(x,t)), \tag{124}$$

$$u_x(x,t) = \frac{1}{2\sqrt{q}}(w(x,t) - z(x,t)). \tag{125}$$

Applying Cauchy–Schwarz inequality, we obtain

$$\begin{aligned}&\|u_t(\cdot,t)\|^2 + \|u_x(\cdot,t)\|^2\\ &\le \frac{L}{2}(\|z(\cdot,t)\|^2 + \|w(\cdot,t)\|^2) + \frac{L}{2q}(\|z(\cdot,t)\|^2 + \|w(\cdot,t)\|^2)\\ &\le \frac{q+1}{2q}L(\|z(\cdot,t)\|^2 + \|w(\cdot,t)\|^2).\end{aligned}$$

The property 3 of Theorem 1 is thus proved.

Realization of the theory result: According to Theorem 1, by applying the control torque $GJU(t)$ to the rotary table of the oil drilling system with the uncertain stick–slip instability and external disturbance at the drilling bit as shown in Fig. 1, the torsional vibration displacement $u(0,t)$ and velocity $u_t(0,t)$ of the drilling bit would be reduced towards zero as time goes on. Note that G, J are constant physical parameters given in Section 2.1. $U(t)$ in (84) includes the adaptive estimations $\hat{c}(t)$, $\hat{a}_j(t)$, $\hat{b}_j(t)$ defined in Section 3, and is constructed by measuring the signals $u(0,t)$, $u_t(0,t)$, $u_t(L,t)$, which are obtained from the acceleration sensor placed at the bit and the feedback signal of the servo actuator at the rotary table, as mentioned in Section 2.1. All signals in the controller are obtained from the direct measurements or integrals without using derivatives, which avoids the measurement noise amplification.

6. Simulation

6.1. Simulation model

The off-shore oil drilling system tested in the simulation is (1)–(3), with the physical parameters shown in Table 1, which are borrowed from Bresch-Pietri and Krstic (2014a) and Sagert et al. (2013). The disturbance at the drill bit is given as a harmonic form of

$$d(t) = 2\cos(2t) + \sin(2t). \tag{126}$$

Therefore, the unknown amplitudes a_1, b_1 in the disturbance are 2,1 respectively. We only know their upper bounds $\bar{a}_1, \bar{b}_1$ are 4,2. The unknown anti-damping coefficient c is 1 and the upper bound is known as $\bar{c} = 2$.

According to Section 2.2-Section 2.3, we know the system (1)–(3) can be written as (13)–(17) where $X(t) = [u(0,t), u_t(0,t)]^T$. The main simulation is conducted based on (13)–(17), and then the responses z, w can be converted to the responses u of the system (1)–(3) through

$$u(x,t) = \frac{1}{2\sqrt{q}}\int_0^x (w(y,t) - z(y,t))dy + u(0,t) \tag{127}$$

by recalling (11)–(12). The finite difference method is adopted to conduct the simulation with the time step and space step as 0.0005 and 0.05, respectively. According to the physical parameters in Table 1, the coefficients in (13)–(17) are obtained as $q = 9.971 \times 10^7$, $k = 9.472 \times 10^6$ through the definitions in Section 2. Consider the initial conditions in (1)–(3) are $u(x,0) = 0.15$, $u_t(x,0) = \sin(\frac{2\pi}{L}x)$. Then the according initial condition in (13)–(17) is $w(x,0) = z(x,0) = \sin(\frac{2\pi}{L}x)$ considering (11)–(12), (127).

Table 1
Physical parameters of the oil drilling system.

Parameters (units)	Values
Length of the drill pipe L (m)	2000
Shear modulus of the drill pipe G (N/m^2)	7.96×10^{11}
Drill pipe moment of inertia per unit of length I_d (kg m)	0.095
Moment of inertia of the BHA I_b (kg m^2)	311
Drill pipe second moment of area J (m^4)	1.19×10^{-5}
Anti-damping parameter c (N m s/rad)	1

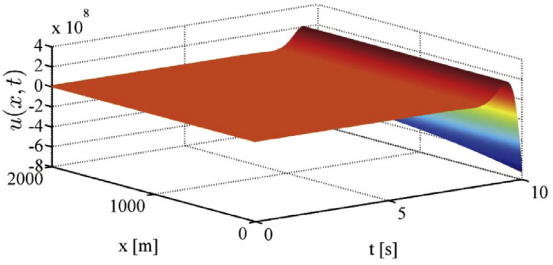

Fig. 3. Open-loop responses of $u(x,t)$.

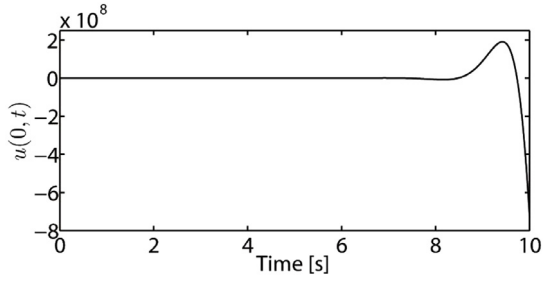

(a) $u(0,t)$.

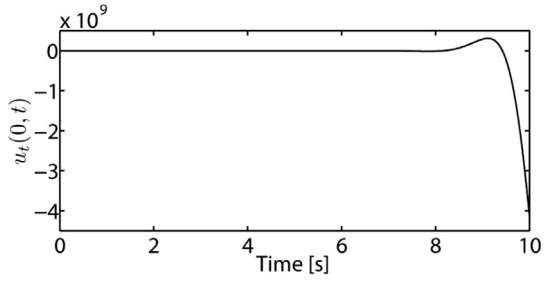

(b) $u_t(0,t)$.

Fig. 4. Open-loop responses of $u(0,t)$, $u_t(0,t)$.

6.2. Open-loop responses

In the open-loop case, it can be seen that the plant (1)–(3) is unstable in Figs. 3–4 because of the effect of the anti-damping at the bit $x = 0$. The according diverging results of $z(x,t)$, $w(x,t)$ (13)–(17) can be seen in Fig. 5. To be exact, the diverging phenomenon starts at $X(t) = [u(0,t), u_t(0,t)]^T$ in (13) (shown in Fig. 4) flowing into $z(0,t)$ via (14) and giving rise to the increase of $|z(0,t)|$, what follows is the diverging response of $z(x,t)$ via (15) and the instability traveling up to the boundary $x = L$, which is shown in Fig. 5(a). According to (17), diverging performance then appears at $w(L,t)$, which leads to the instability of $w(x,t)$ via (16) and causes the increase of $|w(0,t)|$, which is shown in Fig. 5(b).

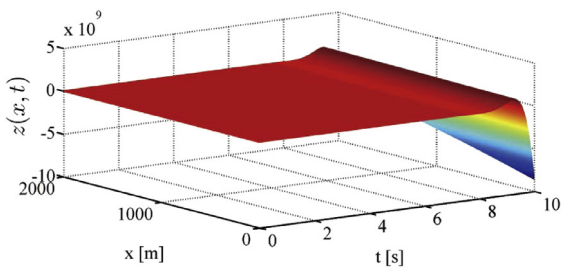

(a) $z(x,t)$.

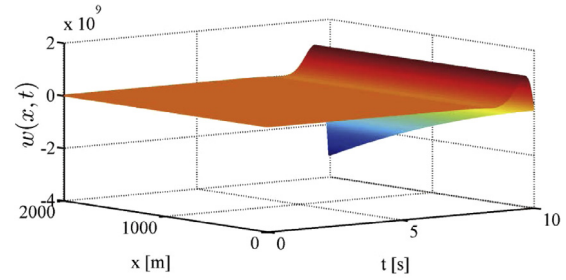

(b) $w(x,t)$.

Fig. 5. Open-loop responses of $z(x,t)$, $w(x,t)$.

6.3. Control law

We apply the control law (84) into (13)–(17), with the control parameters chosen as $\bar{\kappa} = [0.1, 1.5]$, $\gamma_a = 0.005$, $\gamma_b = 0.008$ and $\gamma_c = 0.006$. N in (84) is 1. Note that u_t in (84) can be represented by the states in (13)–(17) via $u_t = \frac{1}{2}(w+z)$. The adaptive estimates $\hat{c}(t), \hat{a}_1(t), \hat{b}_1(t)$ in (84) are calculated from (22) and (25), (23) and (26), (24) and (27). Note that recalling (60)–(61), (40)–(41), (36)–(37), $\int_0^L e^{-x}\alpha(x,t)^2dx$, $\int_0^L e^{x}\beta(x,t)^2dx$ in $\Omega(t)$ (30) of the adaptive estimates also can be represented by the states in (13)–(17):

$$
\begin{aligned}
&\int_0^L e^{-x}\alpha(x,t)^2dx\\
&=\int_0^L e^{-x}(z(x,t)+\Gamma_1(x,t)Z(t))^2dx\\
&=-\int_{t-\frac{L}{\sqrt{q}}}^{t} e^{-\sqrt{q}(t-\delta_1)}\Big(2C_1X(\delta_1)-w(L,\delta_1-\frac{L}{\sqrt{q}})\\
&\quad-\frac{\sqrt{q}}{k}[\hat{a}_1(t),\hat{b}_1(t)]e^{-A_z(t-\delta_1)}Z(t)\Big)^2d\delta_1, \qquad (128)
\end{aligned}
$$

and

$$
\begin{aligned}
&\int_0^L e^{x}\beta(x,t)^2dx\\
&=\int_0^L e^{x}\Big(w(x,t)+\Gamma(x,t)Z(t)\\
&\quad-\int_0^x \phi(x,y,t)(w(y,t)+\Gamma(y,t)Z(t))dy-\gamma(x,t)X(t)\Big)^2dx\\
&=\int_{t-\frac{L}{\sqrt{q}}}^{t} e^{L-\sqrt{q}(t-\delta_1)}\Big[w(L,\delta_1)\\
&\quad+\frac{\sqrt{q}}{k}[\hat{a}_1(t),\hat{b}_1(t)]e^{\frac{A_z}{\sqrt{q}}(L-\sqrt{q}(t-\delta_1))}Z(t)\\
&\quad-\int_{t-\frac{L}{\sqrt{q}}}^{\delta_1}\frac{1}{q}\Big(\bar{\kappa}+\Big[0,\frac{\sqrt{q}\hat{c}(t)}{k}\Big]\Big)\\
&\quad\times e^{(A_E+\hat{A}_c(t)-\frac{1}{\sqrt{q}}BC_1)(\delta_1-\delta_2)}B\\
&\quad\times\Big(w(L,\delta_2)+\frac{\sqrt{q}}{k}[\hat{a}_1(t),\hat{b}_1(t)]e^{\frac{A_z}{\sqrt{q}}(L-\sqrt{q}(t-\delta_2))}Z(t)\Big)d\delta_2\\
&\quad-\Big(\bar{\kappa}+\Big[0,\frac{\sqrt{q}\hat{c}(t)}{k}\Big]\Big)e^{\frac{1}{\sqrt{q}}(A_E+\hat{A}_c(t)-\frac{1}{\sqrt{q}}BC_1)(L-\sqrt{q}(t-\delta_1))}\\
&\quad\times X(t)\Big]^2d\delta_1. \qquad (129)
\end{aligned}
$$

A same process is adopted to calculate $\int_0^L \beta(x,t)dx$ used in (25)–(27).

The controller is activated at $t = \frac{2L}{\sqrt{q}} = 0.4$ s ensuring $\delta_1 - \frac{L}{\sqrt{q}}$ with $\delta_1 \in [t-\frac{L}{\sqrt{q}}, t]$ in $w(L, \delta_1 - \frac{L}{\sqrt{q}})$ in (128) is non-negative.

For comparison, we compare the proposed controller with the classic PD controller which uses the signal $X(t) = [u(0,t), u_t(0,t)]^T$, given by

$$U_{\rm PD}(t) = k_p u(0,t) + k_d u_t(0,t). \qquad (130)$$

The best regulating PD performance is achieved with $k_p = 0.13$ and $k_d = 1.2$ in (13)–(17).

The proposed controller activated at $t = 0.4$ s and the PD controller activated at $t = 0$ s are shown in Fig. 6.

6.4. Closed-loop responses

According to Fig. 7, we know that the responses of $z(x,t)$, $w(x,t)$ under the proposed controller are convergent to a very small neighborhood of zero. From Fig. 8, even though the transient performance of $u(0,t)$, $u_t(0,t)$, i.e., $X(t)$, under the proposed controller is worse than that under the PD controller before about $t = 5.5$ s (the reasons of this phenomenon are shown in Remark 4), the responses of $u(0,t)$, $u_t(0,t)$ under the proposed controller are convergent to a smaller neighborhood of zero than those under the PD controller as time goes on. It physically means the proposed controller has the better suppression performance of the torsional vibration displacement and velocity at the bit. Recalling (127) and the closed-loop responses of $z(x,t)$, $w(x,t)$, $u(0,t)$, the response of $u(x,t)$ under the proposed controller is obtained and shown in Fig. 9, which indicates the torsional vibrations of the oil drilling pipe have been suppressed. The norm $(\|u_t(\cdot,t)\|^2 + \|u_x(\cdot,t)\|^2)^{\frac{1}{2}}$ obtained from (124)–(125) denotes torsional vibration energy consisting of kinetic energy and potential energy. The responses of $(\|u_t(\cdot,t)\|^2 + \|u_x(\cdot,t)\|^2)^{\frac{1}{2}}$ under the proposed controller and the PD controller are shown in Fig. 10. We can see that even though the PD controller has a better transient performance before about $t = 5.5$ s (the reasons of this phenomenon are shown in Remark 4), the proposed controller can reduce the vibration energy to a smaller range around zero as time goes on, which verifies the proposed adaptive controller has the better performance on vibration suppression of the oil drilling pipe in the off-shore oil drilling system.

6.5. Adaptive parameter estimates

The adaptive estimation action is activated at $t = 0.4$ s. From Fig. 11 which shows the adaptive estimation errors of constants c, a_1, b_1 in the above regulation process, we know that the estimations $\hat{c}(t), \hat{a}_1(t), \hat{b}_1(t)$ converge to the values which are very close to the actual ones c, a_1, b_1, as time goes on. Note that even though the estimations do not exactly arrive at their actual values, the state convergence is achieved, which often happens in adaptive control.

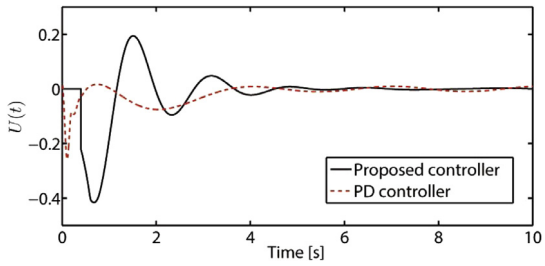

Fig. 6. The proposed control input and the PD control input.

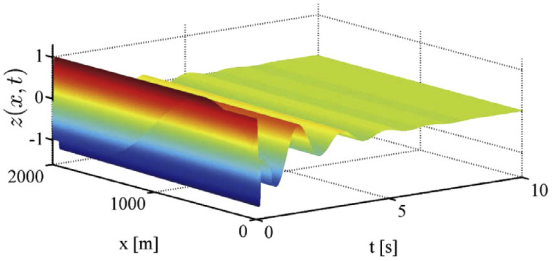

(a) $z(x,t)$.

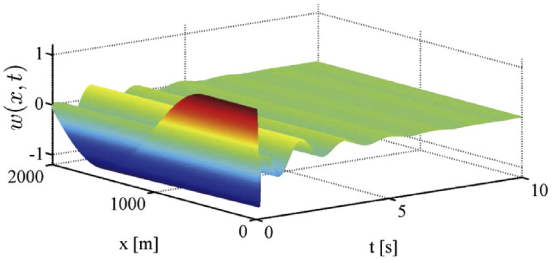

(b) $w(x,t)$.

Fig. 7. Closed-loop responses of $z(x,t)$, $w(x,t)$.

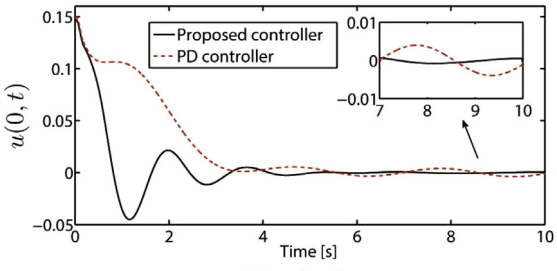

(a) $u(0,t)$.

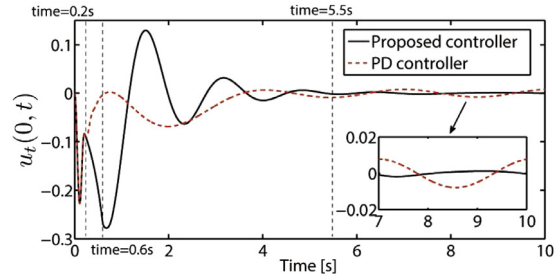

(b) $u_t(0,t)$.

Fig. 8. Closed-loop responses of $X(t) = [u(0,t), u_t(0,t)]^T$ under the proposed adaptive controller and the PD controller, which physically means the torsional vibration angular displacement and velocity at the bit (the reasons of the phenomenon that the PD controller has a better transient performance before about $t = 5.5$ s are illustrated in Remark 4).

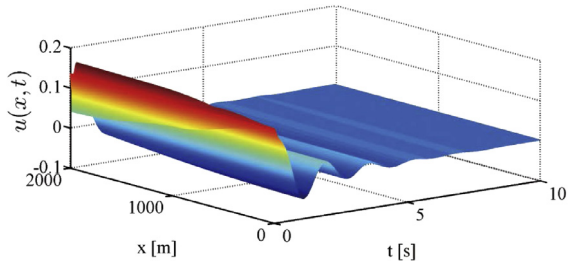

Fig. 9. Closed-loop response of $u(x,t)$, which physically means the torsional vibrations of the oil drilling pipe under the proposed controller.

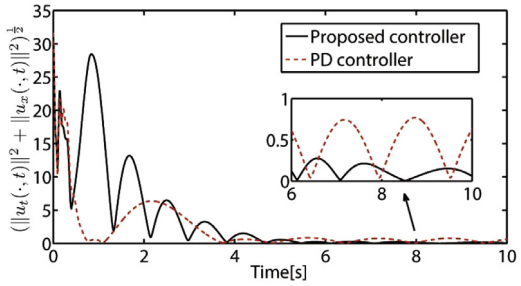

Fig. 10. Closed-loop response of the norm $(\|u_t(\cdot,t)\|^2 + \|u_x(\cdot,t)\|^2)^{\frac{1}{2}}$ in Theorem 1 under the proposed adaptive controller and the PD controller, which physically means torsional vibration energy including kinetic energy and potential energy of the oil drilling pipe (the reasons of the phenomenon that the PD controller has a better transient performance before about $t = 5.5$ s are illustrated in Remark 4).

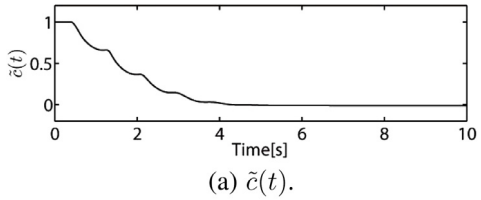

(a) $\tilde{c}(t)$.

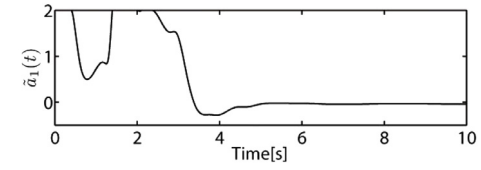

(b) $\tilde{a}_1(t)$.

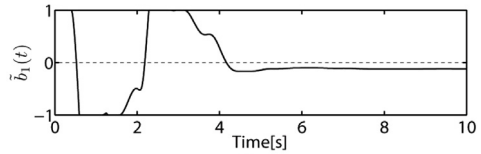

(c) $\tilde{b}_1(t)$.

Fig. 11. Adaptive estimation errors of the anti-damping coefficient c and the disturbance amplitudes a_1, b_1.

Remark 4. There are two reasons of the phenomenon that the PD controller has a better transient performance than the proposed adaptive controller before $t = 5.5$ s. First, the proposed adaptive controller is activated later than the PD controller with a 0.4 s delay. The proposed adaptive controller is activated at $t = 0.4$ s and the regulation action would reach the ODE at $x = 0$ until $t = 0.6$ s because the propagation time from

$x = L$ to $x = 0$ is $\frac{L}{\sqrt{q}} = 0.2$ s in (13)–(17), while the PD controller is activated at $t = 0$ s and regulation action would reach the ODE at $t = 0.2$ s, which can be seen obviously in Fig. 8(b), where the PD controller starts regulating the ODE states towards to zero after $t = 0.2$ s and the response under the proposed adaptive controller continues to deteriorate until about $t = 0.6$ s because of no regulation action to stabilize the anti-stable ODE with the anti-damping term. Second, the PD controller is running under very best parameters which are chosen over many simulation tests (which is equivalent to knowing the model parameters), while the proposed adaptive controller is operating with a poor knowledge of the anti-damping parameter and of the wave amplitude and phase parameters, where the adaptive estimations of the parameters would introduce adaptive learning transient until about $t = 5.5$ s, which can be seen in Fig. 11.

7. Conclusion and future work

In this paper, we present adaptive backstepping control design for a wave PDE system where an anti-damping term with an unknown coefficient and a harmonic disturbance with unknown amplitudes are at the second-order-in-time boundary which is anti-collocated with the control input. The asymptotic convergence of the ODE state, i.e., the uncontrolled boundary states of the wave PDE, and boundedness of all states in the closed-loop system are proved by using Lyapunov analysis. The simulation results verify the effectiveness of the adaptive controller which is used in torsional vibration suppression for an oil drilling system with uncertain stick–slip instability and disturbances at the drilling bit.

The proposed output feedback adaptive controller also can be applied in vibration control of a cable elevator (Wang, Koga, Pi and Krstic, 2018) where the cage is subject to an uncertain cage-guide friction force and an uncertain harmonic airflow disturbance. In the future work, the control design would be extended to the Saint-Venant model (Diagne, Diagne, Tang and Krstic, 2017; Diagne, Tang, Diagne and Krstic, 2017), the representation of which in Riemann coordinates is coupled first-order hyperbolic PDEs including some unstable source terms in the PDE domain (Di Meglio et al., 2018; Di Meglio, Vazquez, & Krstic, 2013; Wang, Krstic and Pi, 2018; Wang, Pi and Krstic, 2018).

References

Aamo, Ole Morten (2013). Disturbance rejection in 2 ×2 linear hyperbolic systems. *IEEE Transactions on Automatic Control*, *58*, 1095–1106.

Abolinia, V. E., & Myshkis, A. D. (1960). A mixed problem for an almost linear hyperbolic system in the plane. *Matematicheskii Sbornik*, *50*, 423–442.

Bekiaris-Liberis, N., & Krstic, M. (2014). Compensation of wave actuator dynamics for nonlinear systems. *IEEE Transactions on Automatic Control*, *59*, 1555–1570.

Bresch-Pietri, D., & Krstic, M. (2014a). Adaptive output feedback for oil drilling stick–slip instability modeled by wave PDE with anti-damped dynamic boundary. In *American control conference*. Portland, Oregon, USA.

Bresch-Pietri, D., & Krstic, M. (2014b). Adaptive output-feedback for wave PDE with anti-damping application to surface-based control of oil drilling stick–slip instability. In *53rd IEEE conference on decision and control*. Los Angeles, California, USA.

Bresch-Pietri, D., & Krstic, M. (2014c). Output-feedback adaptive control of a wave PDE with boundary anti-damping. *Automatica*, *50*, 1407–1415.

Challamel, N. (2000). Rock destruction effect on the stability of a drilling structure. *Journal of Sound and Vibration*, *233*, 235–254.

Detournay, E., & Defourny, P. (1992). A phenomenological model for the drilling action of drag bits. *International Journal of Rock Mechanics, Mining Science and Geomechanical Abstracts*, *29*, 13–23.

Di Meglio, F., Bribiesca, F., Hu, L., & Krstic, M. (2018). Stabilization of coupled linear heterodirectional hyperbolic PDE-ODE systems. *Automatica*, *87*, 281–289.

Di Meglio, F., Vazquez, R., & Krstic, M. (2013). Stabilization of a system of $n+1$ coupled first-order hyperbolic linear PDEs with a single boundary input. *IEEE Transactions on Automatic Control*, *58*, 3097–3111.

Diagne, A., Diagne, M., Tang, S.-X., & Krstic, M. (2017). Backstepping stabilization of the linearized Saint-Venant-Exner model. *Automatica*, *76*, 345–354.

Diagne, M., Tang, S.-X., Diagne, A., & Krstic, M. (2017). Control of shallow waves of two unmixed fluids by backstepping. *Annual Reviews in Control*, *44*, 211–225.

Dunayevsky, V., Abbassian, F., & Judzis, A. (1993). Dynamic stability of drill strings under fluctuating weight on bit. *SPE Drilling and Completion*, *8*, 84–92.

Fossen, T. I. (2011). *Marine craft hydrodynamics and motion control*. New York: Wiley.

Germay, C., Van De Wouw, N., Nijmeijer, H., & Sepulchre, R. (2005). Nonlinear drilling dynamics analysis. *SIAM Journal on Applied Dynamical Systems*, *8*, 527–553.

Guo, W., & Guo, B. Z. (2016). Performance output tracking for a wave equation subject to unmatched general boundary harmonic disturbance. *Automatica*, *68*, 194–202.

Guo, W., Shao, Z. C., & Krstic, M. (2017). Adaptive rejection of harmonic disturbance anticollocated with control in 1D wave equation. *Automatica*, *79*, 17–26.

Jansen, J. D. (1993). *Nonlinear dynamics of oilwell drill strings*. Delft, The Netherlands: Delft University Press.

Karnopp, D. (1985). Computer simulation of stick–slip friction in mechanical dynamic systems. *ASME Journal of Dynamic Systems, Measurement and Control*, *107*, 100–103.

Krstic, M. (2009a). *Delay compensation for nonlinear, adaptive, and PDE systems*. Springer.

Krstic, M. (2009b). Adaptive control of an anti-stable wave PDE. In *Proceedings of the American control conference*. St. Louis, MO, USA.

Krstic, M. (2009c). Compensating a string PDE in the actuation or sensing path of an anti-stable ODE. *IEEE Transactions on Automatic Control*, *54*, 1362–1368.

Krstic, M., Guo, B.-Z., Balogh, A., & Smyshlyaev, A. (2008). Output-feedback stabilization of an anti-stable wave equation. *Automatica*, *44*, 63–74.

Krstic, M., & Smyshlyaev, A. (2008a). *Boundary control of PDEs: A course on backstepping designs*. Singapore: Siam.

Krstic, M., & Smyshlyaev, A. (2008b). Adaptive control of PDEs. *Annual Reviews in Control*, *32*, 149–160.

Landet, I., Pavlov, A., & Aamo, O. (2013). Modeling and control of heave-induced pressure fluctuations in managed pressure drilling. *IEEE Transactions on Control Systems Technology*, *21*, 1340–1351.

Navarro-López, E., & Cortés, D. (2007). Sliding-mode of a multi-DOF oilwell drillstring with stick–slip oscillations. In *Proceedings of the 2007 American control conference* (pp. 3837–3842). New York City, USA.

Richarda, T., Germayb, C., & Detournay, E. (2007). A simplified model to explore the root cause of stick–slip vibrations in drilling systems with drag bits. *Journal of Sound and Vibration*, *305*, 432–456.

Sagert, C., Di Meglio, F., Krstic, M., & Rouchon, P. (2013). Backstepping and flatness approaches for stabilization of the stick–slip phenomenon for drilling. *IFAC Proceedings Volumes*, *46*(2), 779–784.

Saldivar, B., Boussaada, I., Mounier, H., & Mondie, S. (2014). An overview on the modeling of oilwell drilling vibrations. *IFAC Proceedings Volumes*, *47*(3), 5169–5174.

Saldivar, B., & Mondiš, S. (2013). Drilling vibration reduction via attractive ellipsoid method. *Journal of the Franklin Institute*, *350*, 485–502.

Saldivar, B., Mondiš, S., Loiseau, J. J., & Rasvan, V. (2013). Suppressing axial torsional coupled vibrations in oilwell drill strings. *Journal of Control Engineering and Applied Informatics*, *15*, 3–10.

Saldivar, B., Mondiš, S., Niculescu, S. I., Mounier, H., & Boussaada, I. (2016). A control oriented guided tour in oilwell drilling vibration modeling. *Annual Reviews in Control*, *42*, 100–113.

Serrarens, A. F. A., van de Molengraft, M. J. G., Kok, J. J., & van den Steeen, L. (1998). H∞ Control for suppressing stick–slip in oil well drill strings. *IEEE Control Systems*, *18*, 19–30.

Su, L., Wang, J. M., & Krstic, M. (2018). Boundary feedback stabilization of a class of coupled hyperbolic equations with non-local terms. *IEEE Transactions on Automatic Control*, *63*, 2633–2640.

Tang, S.-X., Guo, B.-Z., & Krstic, M. (2014). Active disturbance rejection control for 2 ×2 hyperbolic systems with input disturbance. In *IFAC world congress* (pp. 1027–1032).

Tang, S.-X., & Xie, C. (2011). State and output feedback boundary control for a coupled PDE-ODE system. *Systems & Control Letters*, *60*, 540–545.

Wang, J., Koga, S., Pi, Y., & Krstic, M. (2018). Axial vibration suppression in a PDE model of ascending mining cable elevator. *ASME Journal of Dynamic Systems, Measurement and Control*, *140*, 111003.

Wang, J., Krstic, M., & Pi, Y. (2018). Control of a 2 ×2 coupled linear hyperbolic system sandwiched between two ODEs. *International Journal of Robust and Nonlinear*, *28*, 3987–4016.

Wang, J., Pi, Y., & Krstic, M. (2018). Balancing and suppression of oscillations of tension and cage in dual-cable mining elevators. *Automatica*, *98*, 223–238.

Wang, J., Tang, S.-X., Pi, Y., & Krstic, M. (2018). Exponential anti-collocated regulation of the disturbed cage in a wave PDE-modeled ascending cable elevator. *Automatica*, *95*, 122–136.

Zhang, S., He, W., & Ge, S. S. (2012). Modeling and control of a nonuniform vibrating string under spatiotemporally varying tension and disturbance. *IEEE/ASME Transactions on Mechatronics*, *17*, 1196–1203.

Zhou, Z., & Tang, S.-X. (2012). Boundary stabilization of a coupled wave-ODE system with internal anti-damping. *International Journal of Control*, *85*, 1683–1693.

Ji Wang received the Ph.D. degree in Mechanical Engineering in 2018 from Chongqing University, Chongqing, China. He is currently a Postdoctoral Scholar-Employee in the Department of Mechanical and Aerospace Engineering at University of California, San Diego, La Jolla, CA, USA. His research interests include modeling and control of distributed parameter systems, active disturbance rejection control and adaptive control, with applications in cable-driven mechanisms.

Shu-Xia Tang received her Ph.D. in Mechanical Engineering in 2016 from the Department of Mechanical & Aerospace Engineering, University of California, San Diego, USA. She is currently an assistant professor at the Department of Mechanical Engineering, Texas Tech University, USA. She is an IEEE senior member and is an IEEE CSS (Control Systems Society) Technical Committee member on Distributed Parameter Systems. She serves as an associate editor of Journal of Control, Automation and Electrical Systems and as an IEEE CSS Conference Editorial Board member. Her main research interests are stability analysis, estimation and control design of distributed parameter systems.

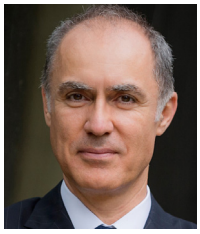

Miroslav Krstic is Distinguished Professor of Mechanical and Aerospace Engineering, holds the Alspach endowed chair, and is the founding director of the Cymer Center for Control Systems and Dynamics at UC San Diego. He also serves as Senior Associate Vice Chancellor for Research at UCSD. As a graduate student, Krstic won the UC Santa Barbara best dissertation award and student best paper awards at CDC and ACC. Krstic has been elected Fellow of seven scientific societies – IEEE, IFAC, ASME, SIAM, AAAS, IET (UK), and AIAA (Assoc. Fellow) – and as a foreign member of the Serbian Academy of Sciences and Arts and of the Academy of Engineering of Serbia. He has received the SIAM Reid Prize, ASME Oldenburger Medal, Nyquist Lecture Prize, Paynter Outstanding Investigator Award, Ragazzini Education Award, IFAC Nonlinear Control Systems Award, Chestnut textbook prize, Control Systems Society Distinguished Member Award, the PECASE, NSF Career, and ONR Young Investigator awards, the Schuck ('96 and '19) and Axelby paper prizes, and the first UCSD Research Award given to an engineer. Krstic has also been awarded the Springer Visiting Professorship at UC Berkeley, the Distinguished Visiting Fellowship of the Royal Academy of Engineering, and the Invitation Fellowship of the Japan Society for the Promotion of Science. He serves as Editor-in-Chief of Systems & Control Letters and has been serving as Senior Editor in Automatica and IEEE Transactions on Automatic Control, as editor of two Springer book series, and has served as Vice President for Technical Activities of the IEEE Control Systems Society and as chair of the IEEE CSS Fellow Committee. Krstic has coauthored thirteen books on adaptive, nonlinear, and stochastic control, extremum seeking, control of PDE systems including turbulent flows, and control of delay systems.